NASA CONTRACTOR REPORT

NASA CR-15

NASA CR-1531

STUDY OF A WATER-VAPOR ELECTROLYSIS UNIT

by J. E. Clifford, B. C. Kim, and E. S. Kolic

Prepared by
BATTELLE MEMORIAL INSTITUTE
Columbus, Ohio
for Ames Research Center

NATIONAL AERONAUTICS AND SPACE ADMINISTRATION • WASHINGTON, D. C. • MARCH 1970

NASA CR-1531

Mar 70

STUDY OF A WATER-VAPOR ELECTROLYSIS UNIT

added E; T; Water-vapor ... unit.

unit -By J. E. Clifford, B. C. Kim, and E. S. Kolic

Prepared under Contract No. NAS 2-2156 by desc. only
Corp. author -BATTELLE MEMORIAL INSTITUTE
Columbus, Ohio

for Ames Research Center

NATIONAL AERONAUTICS AND SPACE ADMINISTRATION

For sale by the Clearinghouse for Federal Scientific and Technical Information
Springfield, Virginia 22151 – CFSTI price $3.00

FOREWORD

The research reported here was performed at Battelle Memorial Institute, Columbus Laboratories, Columbus, Ohio from 23 April 1968 to 1 February 1969, under Contract No. NAS 2-2156. This research was part of a larger program in the area of water vapor electrolysis. During the course of the Battelle effort which began in June 1964, two other contractor reports were generated (CR 711 and CR 73170).

An essential requirement for a life support subsystem for long duration manned space missions is the ability to convert human waste products into some useful products. The water vapor electrolysis cell recovers oxygen for breathing from waste water vapor arising from respiration and perspiration. In addition to oxygen recovery the vapor cell aids in cabin humidity control and also provides hydrogen for the reduction of metabolic carbon dioxide. The object of this program was to develop a reliable and efficient water vapor electrolysis unit capable of performing these functions. Size and weight optimization and minimum power requirements were of prime consideration.

The technical data which was derived from theoretical analyses and experimental tests will be applied to the design and fabrication of flight prototype hardware.

Funding for this effort was provided by the Biotechnology and Human Research Division, NASA Office of Advanced Research and Technology, Washington, D. C. The technical monitor for this contract was Ezekiel L. Smith with the assistance of Dr. Theodore Wydeven, Environmental Control Research Branch, NASA-Ames Research Center, Moffett Field, California.

Ezekiel L. Smith

Ezekiel L. Smith
Research Scientist
Environmental Control Research Branch

ABSTRACT

Continuing development of the acid-type water-vapor electrolysis concept for oxygen generation was directed toward interface factors for subsystem integration in advanced life support systems. The experimental program involved detailed analysis of product gas purity. The sulfuric acid type water-vapor electrolysis module (1/4-man capacity) provided by Ames Research Center had already completed 100 days of satisfactory operation at design conditions. During an additional 45 days of evaluation on this program, it was established that the small generation rate of ozone and acid spray could be controlled to well below the acceptable limits for continuous exposure by use of the usual charcoal and particulate filters used for trace-contaminant control. No other trace contaminants of concern were found in the oxygen (air) or hydrogen at a level of detection of 0.01 ppm. There was preliminary evidence that airborne bacteria were rapidly destroyed. Supplemental data on current/voltage relationships for individual cells of the module was obtained.

TABLE OF CONTENTS

TABLE OF CONTENTS
(Continued)

LIST OF FIGURES

LIST OF TABLES

LIST OF TABLES
(Continued)

STUDY OF A WATER-VAPOR ELECTROLYSIS UNIT

by

J. E. Clifford, B. C. Kim, and E. S. Kolic

SECTION 1. INTRODUCTION AND SUMMARY

The water-vapor electrolysis cell concept that has resulted from prior work (1-5)* has reached a status of acceptance as a new approach worthy of serious consideration for advanced life-support systems. The objective of the present study is to define the optimum water-vapor electrolysis subsystem design in anticipation of future flight-prototype development. Specifically, the tasks in this program call for study and analysis of electrolysis-cell operation and interface problems related to integration of the water-vapor electrolysis cell in advanced life-support systems. One important area of evaluation of electrolysis-cell operation is concerned with investigation of trace contaminants generated from electrolysis-cell operation. This report covers experimental work performed on gas purity using an electrolysis module provided by the sponsor. The water-vapor electrolysis module contains 12 cells (of the sulfuric acid/silica gel matrix design) that had completed over 100 days of operation on room air at NASA Ames Research Center. An additional 45 days of operation (over a 90-day period) under controlled air conditions was obtained in the experiments at Battelle-Columbus. The module was still operable at the nominal capacity of 1/4-man (0.5 lb O_2/day) as designed for operation on air of 75 F and 50 percent relative humidity at an average cell voltage of 2.15 volts/cell.

The results of the gas-purity study indicated that there should be no problem in normal operation of an acid-type water-vapor electrolysis unit directly on cabin air in the open-loop mode utilizing the filters that are normally available for trace-contaminant control. The maximum ozone generation for slightly "off-normal" operation at an average cell voltage of 2.20 volts/cell was 5 ppm** based on oxygen produced*** for this particular module. Experiments demonstrated that typical activated charcoal filters as normally used could maintain the ozone concentration at least an order of magnitude lower than the accepted spacecraft limit of 0.02 ppm for extended continuous exposure.**** Similarly, the acid spray level of up to 1.4 ppm could be maintained below 0.00001 ppm by the use of typical particulate filters (0.3μ) as normally used in space cabin simulators. No other trace contaminants of concern were detected in the oxygen from either the electrolysis operation or outgassing of the module. No sulfur compounds of other trace contaminants of significance were detected in the hydrogen gas produced. The results of the gas purity investigation in this study are meaningful because the experimental setup and analytical techniques used provided for a low limit of detection (i.e. ozone, 0.0025 ppm; acid, 0.00001 ppm; and other compounds 0.01 ppm by mass

*References are listed in Section 4 of this report.

**Ppm on a mole basis.

***Reported on the basis of oxygen produced to define generation rate in terms of electrolytic oxygen generation rate.

****Trace-contaminant limits in this report refer to the 90-day limits established by the National Academy of Sciences, National Research Council, Space Science Board.(10)

spectrometer). In addition, results are significant because they are related to an electrolysis unit that had demonstrated satisfactory extended operation.

Exploratory studies on injection of contaminants into the closed-loop experimental apparatus indicated that airborne microorganisms are destroyed rapidly by the electrolysis-unit operation. However, there was no indication that injected carbon monoxide or methane at initial concentrations of about 100 ppm in air was oxidized by electrolysis-cell operation. More readily oxidizable hydrogen was already present at various levels from 500 to 1200 ppm in the air recirculated in the closed loop. The source of the minor hydrogen leakage (crossleak of matrix or external porting) could not be identified because the entire module was enclosed in the 3 ft^3 box forming the closed loop.

In view of satisfactory extended performance of the water-vapor electrolysis module, the last 5 days of operation were directed toward identification of current/voltage relationships as related to individual cell performance under controlled conditions. Therefore, it was necessary to reconnect the 12 cells in series from the previous series/parallel arrangement with 4 cells in parallel.

Higher-than-average voltage was measured on the cells at either end of the module which indicated some factor associated with their location in the module. However, the problem corrected itself with a significant reduction in ozone generation to 0.07 ppm. During 24 hours of operation at 48±2 percent relative humidity (75 F), which is close to design conditions, the voltage performance of all cells was very good (2.14 ± 0.08 volts) at the nominal 1/4-man rate. However, the analysis of the data indicated the desirability of the usual design practice of having two or more cells connected in parallel for each series connected group in the module.

For operation at a lower humidity of 40 ± 2 percent (75 F), it was necessary to reduce the current density by about 25 percent. The problem of operation on low humidity appears to correlate with observations during the first 100 days of operation. The current/voltage data describing cell voltage characteristics provided correlation of anode overvoltage, ozone production and cell polarization, which appears to be consistent with prior observations on sulfuric acid electrolyte for water-vapor electrolysis. The supplemental information on cell performance included as Appendix B of this report includes current/voltage data on each cell of the module. Appendix A contains a derivation of heat- and mass-transfer relationships applicable to water-vapor electrolysis which are useful in interpreting cell performance.

In addition to the experimental studies, the factors involved in system integration of the water-vapor electrolysis concept are discussed in Section 3 of this report. Principal attention was given to potential interface problems such as hydrogen delivery pressure to carbon dioxide-reduction subsystems, electrical power supply voltage/current regulation, thermal control, source of water or water vapor, auxiliary control requirement and operating limits for water-vapor electrolysis cells. Operational reliability, system complexity, and safety aspects of air versus oxygen are also factors that might influence a choice of open-loop or closed-loop operation, a choice of electrolyte, or a choice of matrix design.

There were several possible solutions indicated for every potential interface problem and the available information is sufficient to begin flight prototype development.

However, to assist in defining the solutions that would provide the best utilization of the water-vapor electrolysis concept, further research should provide data relating to the effect of cabin decompression, the effect of differential gas pressure on matrix design and cell performance, and the effect of operation over wider limits of temperature, humidity, air flow, and current density, as related to the matrix/electrolyte design.

SECTION 2. TRACE-CONTAMINANT STUDIES

INTRODUCTION

While the technical means of control of atmospheric trace contaminants generated by electrolysis cells are known, quantitative data on generation rates are needed to estimate the penalty for control in terms of added electrical power for circulating air, fixed weight of filter and adsorbent beds, and expendable weight of filters and adsorbents. An experimental program was required to obtain these quantitative data. In particular, the present study was required because prior research on the water-vapor electrolysis cell at Battelle and Ames Research Center had called attention to the technical fact that trace contaminants can be present in electrolytically generated gases.

Misleading conclusions might be reached by referring to electrolytically produced gas analyzing 99.95 percent oxygen as "high gas purity". Similarly, "excellent gas purity" is inferred from the absence of detectable trace contaminants in the gas analyzed with a mass spectrograph with a limit of detection of 0.02 percent by volume. Since 0.02 percent is about equivalent to 200 ppm, a large number of potential contaminants with lower acceptable limits cannot be assumed to be absent merely because they were below the limit of detection for the analytical equipment. The orders of magnitude involved in reporting gas purity in percent rather than ppm can be illustrated for electrolyte entrainment in oxygen produced by aqueous electrolysis cells. The limit for such electrolyte compounds as NaOH, KOH, H_3PO_4, and H_2SO_4 is probably about 0.1 ppm for continuous exposure, which would require an oxygen purity of 99.99999 percent.

Obviously, a high degree of analytical accuracy is required to verify the purity of electrolytically generated oxygen that will be added to the cabin atmosphere for continuous metabolic consumption by man. In the present study, the limits of detection were 0.00001 ppm for acid, 0.0025 ppm for ozone, and 0.01 ppm (obtained by mass spectrometer analysis) for other compounds including outgassing products from materials of construction of the electrolysis unit. The latter limit of detection of 0.01 ppm is sufficiently low that it can be assumed that undetected compounds would not accumulate to a critical concentration even if no specific control means were provided for the contaminant.

In the case of ozone and acid spray, which on the basis of prior research were suspected of being at levels requiring treatment, quantitative data were needed on contaminant generation rates under known operating conditions of the water-vapor electrolysis unit. A further objective of the studies was to verify that ozone and acid spray could be controlled to acceptable levels by typical filtering equipment already in use to control trace contaminants in man-rated space-cabin simulators.

WATER-VAPOR ELECTROLYSIS MODULE

The water-vapor electrolysis unit used in this study (Figure 1) was provided by Ames Research Center and will be referred to in this report as the ARC module. The

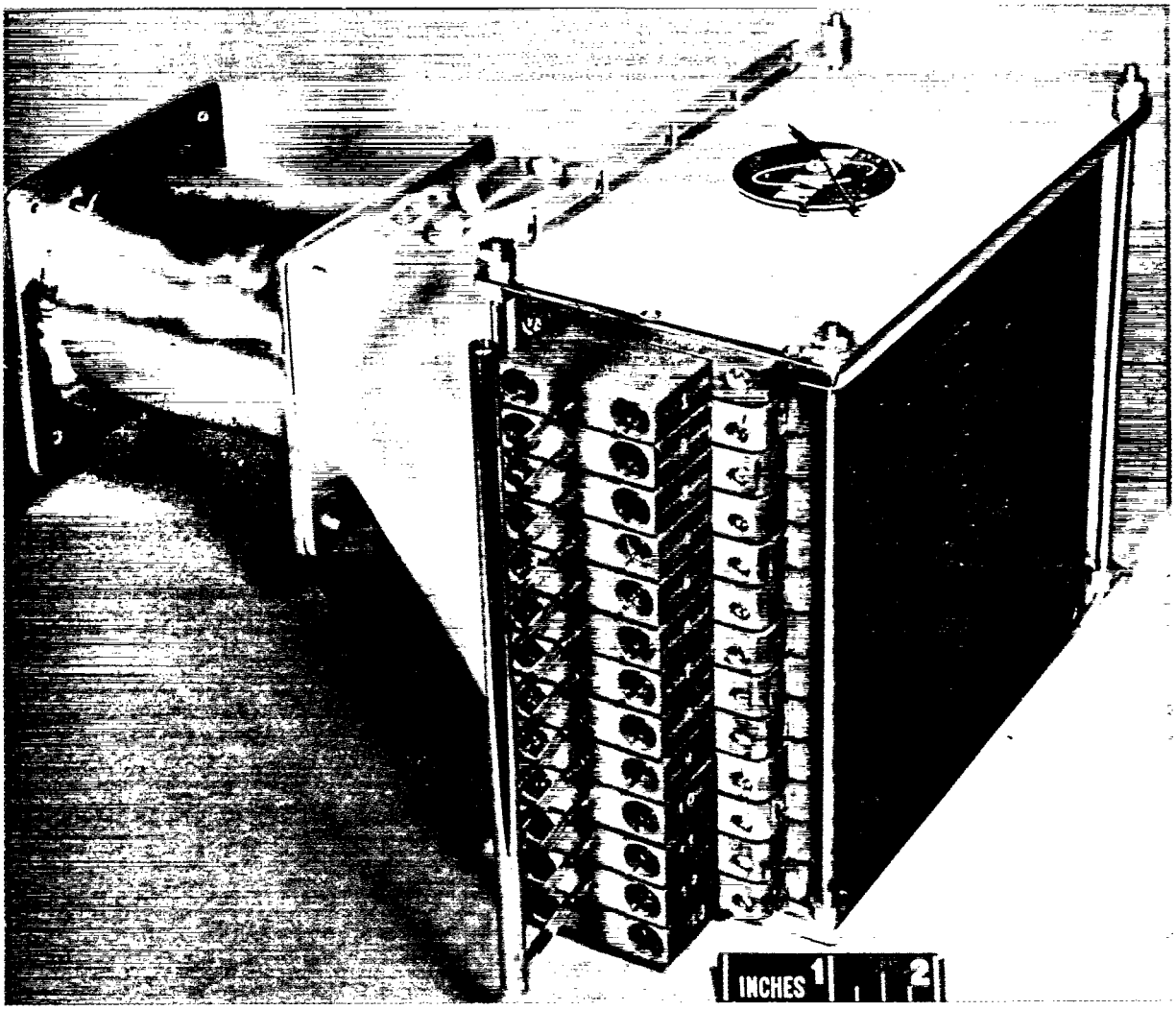

FIGURE 1. AMES RESEARCH CENTER WATER-VAPOR ELECTROLYSIS MODULE OF NOMINAL 1/4-MAN CAPACITY

design of the ARC module has been described previously[1, 2]* and is distinguished by the use of sulfuric acid electrolyte immobilized in a matrix of silica gel on either side of a microporous polyvinylchloride (PVC) membrane. The ARC module consists of 12 single cells (11 in.^{2}/cell) and, when operated at the nominal design current density of 34.7 amp/ft^2, has a 1/4-man capacity (0.5 lb O_2/day).

Immediately prior to the present studies on gas purity at Battelle, the ARC module had completed 100 days of evaluation at Ames Research Center on room air. (The results of the latter evaluation are being prepared for publication.) During the 100-day evaluation, the cells of the module were connected electrically in a series/parallel arrangement consisting of three groups of cells connected in series and four cells in each group connected in parallel:

Group 1 (Cells 1, 2, 3, 4)

Group 2 (Cells 5, 6, 7, 8)

Group 3 (Cells 9, 10, 11, 12).

The above series/parallel arrangement was retained for the gas-purity studies at Battelle to provide a direct correlation with prior results at Ames Research Center. The ARC module was designed for normal operation with air at 75 F and 50 percent relative humidity. With adequate air flow ($n \geq 20$), the rated capacity of 1/4-man could be obtained under normal conditions with an imposed voltage of 6.45 volts. Off-normal operation at an imposed voltage of 6.60 volts was also evaluated with respect to ozone generation. The above operational performance values had been established during the 100-day evaluation at Ames Research Center under representative operational conditions of varying temperatures and humidity.

The verification of nominal design performance at Battelle under controlled temperature (75 ± 0.5 F) and relative humidity (50 ± 2 percent) provided added value and significance to the gas-purity results based on an electrolysis unit which had already operated successfully for 100 days.

EXPERIMENTAL APPARATUS AND PROCEDURE

Closed-Loop Apparatus for Trace-Contaminant Identification

Experimental apparatus assembled for trace-contaminant studies is shown schematically in Figure 2. The electrolysis unit was enclosed in a box to permit the contaminants generated from electrolysis-cell operation to build up to measurable levels. The rectangular box (1 foot high, 1.5 feet wide, and 2 feet long) was fabricated from stainless steel and sealed at front and back with glass plates. Silicone-rubber and stainless-steel tubings were used throughout to minimize decomposition of ozone generated from electrolysis-cell operation.

*References are listed in Section 4.

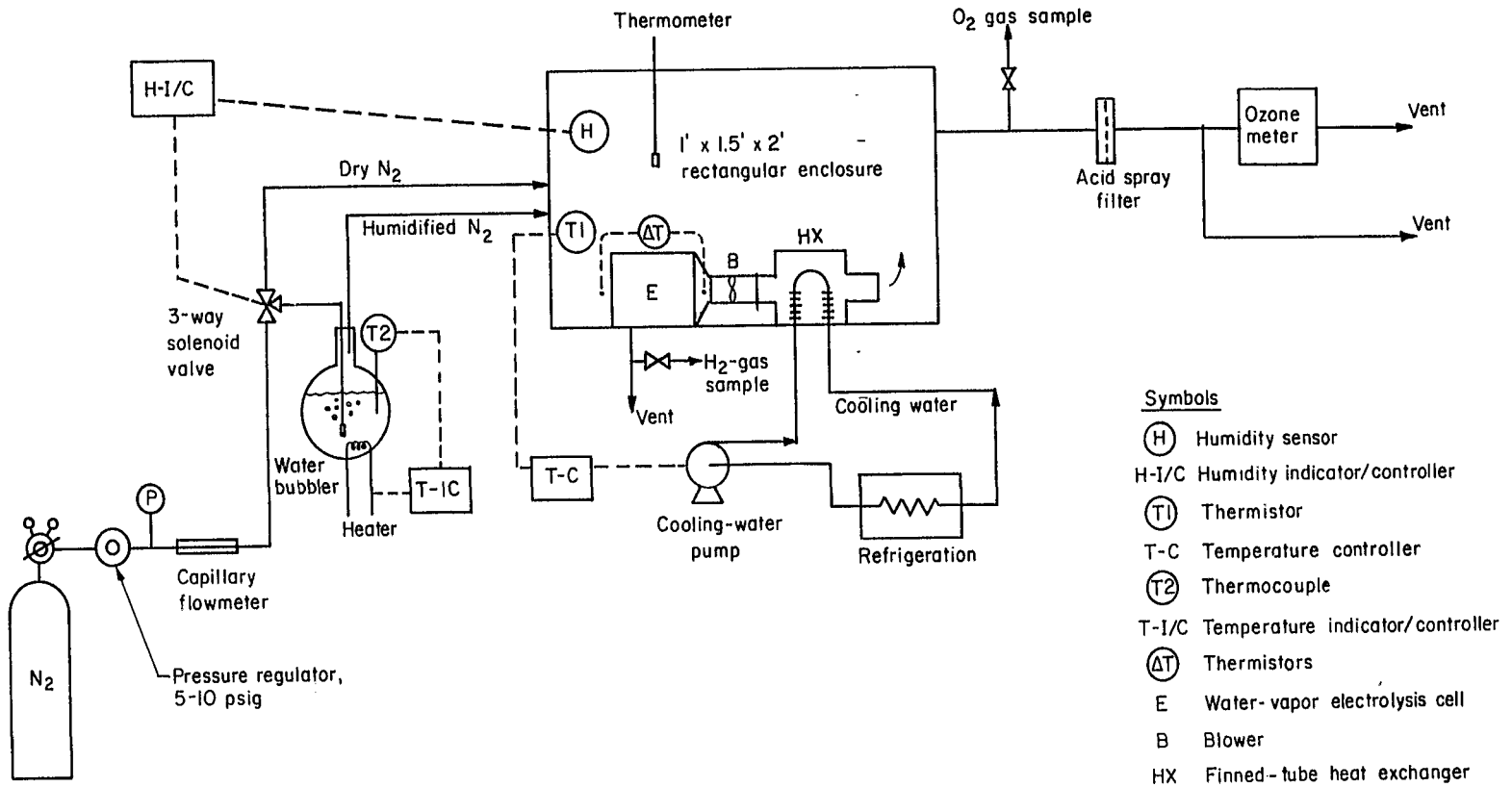

FIGURE 2. EXPERIMENTAL APPARATUS FOR TRACE-CONTAMINANT STUDIES

Temperature and Humidity Measurement and Control

The temperature inside the box was controlled by a thermistor and a temperature controller that regulated flow of cooling water through the heat exchanger. The heat exchanger was a finned-tube type, constructed from aluminum. The anodic gas at the inlet of the electrolysis unit was controlled at 75 ± 0.5 F.

Since one objective of the study was to determine contaminant generation rates, the choice of method of humidity control was important. Recycle of the box atmosphere through a humidifier (i.e., water bath or silica gel column) was avoided to minimize uncontrolled adsorption of contaminants.

The humidity inside the box was controlled by regulating water-vapor feed, using nitrogen as a carrier gas. The water-vapor feed was regulated automatically by means of a three-way solenoid valve that passed either dry or humidified nitrogen when activated by a humidity indicator/controller. Nitrogen was humidified by passing it through a water bubbler maintained at about 190 F. The nitrogen feed was present at approximately four times the rate of oxygen production to maintain a gas composition of about 4:1 nitrogen-oxygen mixture inside the box on the anodic side.

The increase of the anodic-gas temperature in passing through the electrolysis cell was measured using two thermistors located at the inlet and the outlet of the cell. Measurement accuracy of the differential temperature was ±0.1 F. The differential temperature measurement (ΔT) is a convenient method of controlling the airflow through the cell, and the ΔT value can be used to calculate the relative airflow parameter (n) by use of suitable equations.[4]

Electrical Control Circuits

A schematic of the electrical penetrations of the box is shown in Figure 3. To protect the electrolysis cell from possible damage during unattended operation, the electrical circuiting was designed to shut the system down if a critical parameter value exceeded preset limits. Schematics illustrating the circuiting of the electrical components are shown in Figure 4. Operation of the components is also described in Figure 4.

Trace-Contaminant Identification and Measurement

Calculation of Contaminant Generation Rate

Since the gas-phase volume of the electrolysis unit on the anodic side includes the void space inside the experimental box which is large compared to the volume of oxygen generated over a short period of time, the level of contaminant generated from water electrolysis is expected to build up slowly inside the box. By allowing the electrolysis unit to operate over a sufficiently long period of time, the contaminant level can be built up close to its maximum steady-state value for sampling and analysis. Gas analysis should then provide the rate of contaminant generation and the concentration of contaminant in the oxygen generated from water electrolysis.

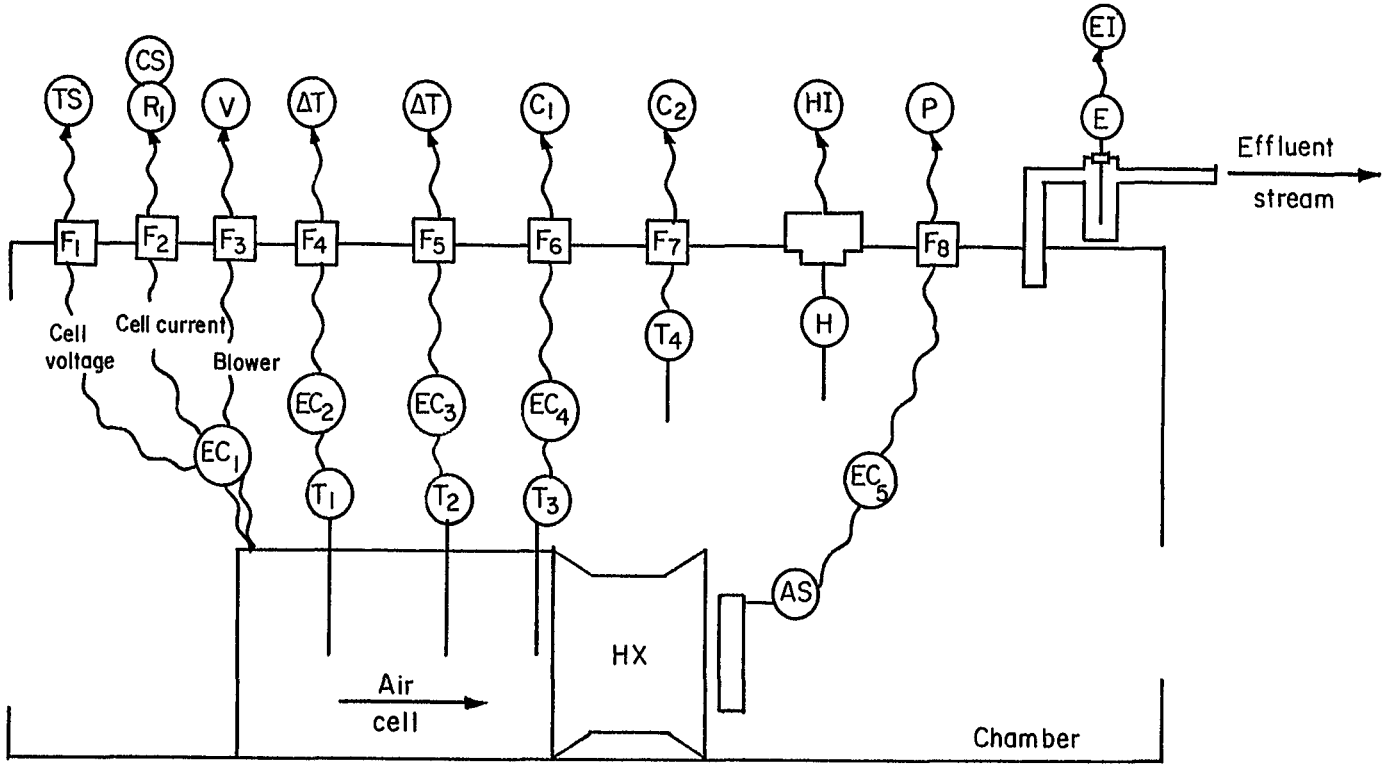

EC	Electrical connector	V	Variac	HI	Humidity indicator
F	Electrical feed-through	T	Thermistor probe	AS	Airflow switch
TS	Terminal switch box	ΔT	Differential-temperature indicator	E	Explosive-mixture probe
R	Rectifier	C	Thermistor controller	EI	Explosive-mixture indicator
CS	High-current switch	H	Humidity probe	P	Parameter controller

FIGURE 3. SCHEMATIC OF ELECTRICAL PENETRATIONS

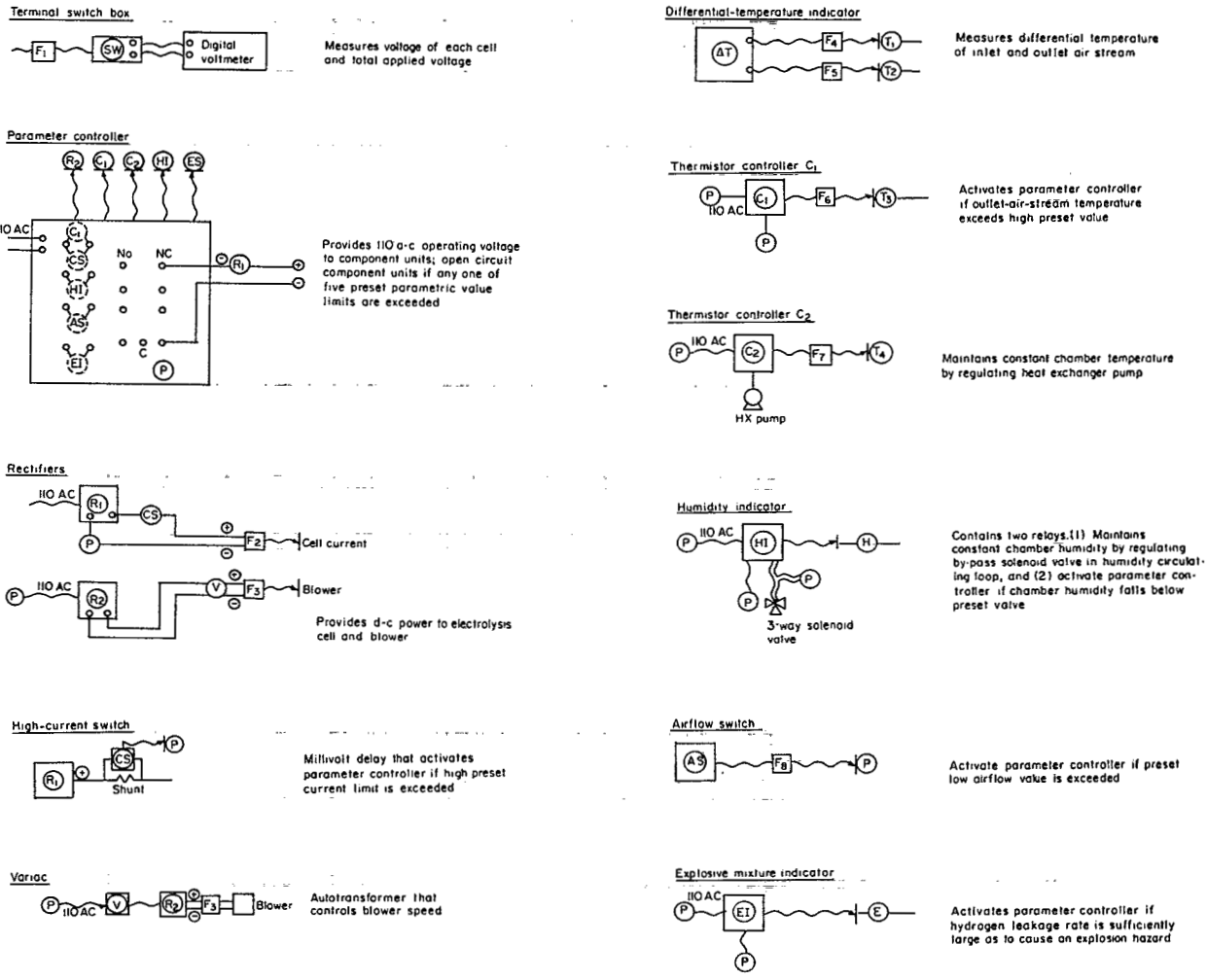

FIGURE 4. CIRCUITRY OF ELECTRICAL COMPONENTS AND DESCRIPTION OF FUNCTION

The contaminant level and the rate of contaminant generation are related as a function of electrolysis-cell operating time by the following equation:

$$m - vc = V \frac{dc}{dt} \quad , \tag{1}$$

where

c = concentration of contaminant in anodic gas, g-moles/ft^3

m = rate of contaminant generation, g-moles/hr

v = rate of anodic-gas output, ft^3/hr

V = total volume of anodic gas inside box, ft^3

t = cell-operating time, hr.

The solution of Equation (1) yields the level of contaminant buildup as function of electrolysis-cell operating time.

$$c = \frac{m}{v} \left\{ 1 - \exp \left(\frac{-vt}{V} \right) \right\} . \tag{2}$$

The steady-state concentration (c_∞) can be obtained from Equation (2) as follows:

$$c_\infty = \frac{m}{v} . \tag{3}$$

The rate whereby the contaminant builds up to its ultimate steady-state level depends on the parameter v/V. The parameter can be estimated for the present experimental set-up as follows:

v = 1.59 ft^3/hr

V = (3 - 0.5) ft^3 = 2.5 ft^3, assuming the volume of equipment inside the box to be 0.5 ft^3

v/V = 0.637 hr^{-1}.

The contaminant buildup as a function of electrolysis-cell operating time would be as follows:

t, hr	c/c_∞
0	0
1	0.472
5	0.959
10	0.998

The results indicate that the contaminant would build up to 95.9 percent of its ultimate steady-state level after 5 hours of electrolysis-cell operation. The anodic-gas samples for analysis of trace contaminants should be taken after about 5 hours of operation at given operating conditions to obtain a reliable estimate of the steady-state concentration.

The rate of contaminant generation can be calculated from the estimated steady-state concentration by using Equation (3). Since approximately 4 volumes of nitrogen are added for each volume of oxygen generated in the anodic side, the concentration of contaminant on the basis of the oxygen generated would be as follows:

$$c_o = 5\, c_\infty \quad . \tag{4}$$

The steady-state concentration (c_∞) must not exceed one-fifth of the maximum acceptable concentration if the cabin atmosphere is 100 percent oxygen or the maximum acceptable concentration if the cabin atmosphere is 20 percent oxygen.

Analysis for Ozone

The effluent from the anodic side (mostly nitrogen and oxygen) of the electrolysis unit was analyzed for ozone by passing a portion of the effluent through a MAST ozone analyzer (Model 724-2). The Mast analyzer puts out 20 microamperes of signal for 1 ppm of ozone in the gas being analyzed. A Sargent recorder (Model S-72150) used for measurement has a sensitivity of 0.025 microampere, which corresponds to 0.00125 ppm ozone. However, the lower limit of detection for ozone was taken as 0.0025 ppm in this study since analysis of the dry-cylinder nitrogen with the MAST ozone analyzer indicated 0.0025 ppm of ozone.

The reliability of the MAST ozone analyzer was checked against a wet-chemical analysis. In the wet-chemical method, ozone was collected in a 2 N KI solution by bubbling a total of 80 liters of the anodic gas through the solution over a 4-hour period. During this period, the ozone concentration in the anodic gas measured with the MAST analyzer was 1.4 ppm. To determine the total ozone collected, the KI solution was acidified with dilute sulfuric acid and titrated with a 0.01 N $Na_2S_2O_3$ solution, using starch as an indicator.[6] The wet-chemical analysis indicated 0.19 mg of total ozone, which agreed with 0.20 mg obtained with the MAST analyzer. It was concluded that the ozone determination by the MAST analyzer was reliable in the indicated range.

Analysis for Acid Spray

The concentration of acid sprays in the anodic gas was determined by first passing the effluent from the box through a filter to trap the acid sprays. The filter is a glass-fiber felt, Type MSA 1106B, obtained from Mine Safety Appliance. Filtering efficiency is greater than 99.9 percent for particle sizes greater than 0.3 micron.[7] Acid determination was performed by dispersing the filter in 50 ml of deionized water and titrating the dispersion with a 0.01 N sodium hydroxide solution using a pH meter for end-point determination.

The pH change of the dispersion was used for estimating extremely small acid concentrations. In one 88-hour collection, a pH change of only 0.1 was found between a blank filter and the filter used to collect the acid spray for analysis. The lower limit of detection of acid of 1×10^{-5} ppm was calculated by assuming conservatively a pH unit of 0.4 as the accuracy of pH measurement.

Mass-Spectrometer Analysis

The gases on the anodic and cathodic sides of the electrolysis unit were sampled directly from the box and scanned on a mass spectrometer to identify gaseous contaminants other than ozone and acid sprays. Of particular interest were sulfur compounds that might originate from electrolysis with sulfuric acid electrolyte and organic compounds that might originate from the polyvinylchloride used in the electrolysis-cell structure (including outgassing).

Trace-Contaminant Control With Charcoal and Particulate Filters

Following trace-contaminant identification, experiments were performed with filters to demonstrate the degree of contaminant control attainable. An activated-charcoal filter and a particulate filter were installed at the outlet of the heat exchanger as shown in Figure 5. The charcoal filter was intended for ozone removal and the particulate filter for removal of acid sprays generated from electrolysis-cell operation. The two filters were connected in series, the particulate filter ahead of the charcoal filter to remove acid sprays prior to passing the anodic gas through the latter for ozone removal. Both filters are of the same type used in the ILSS at the NASA Langley Research Center.(8)

The particulate filter was purchased from Flanders Filters, Inc., and is designated as 6C-33G-Size A. The filter is rated for an airflow of 25 cfm (NTP) and a pressure drop of 1 inch water. The filter medium is a glass-fiber felt without binder. The outside dimensions are 8 x 8 inches in cross section and 3-1/6 inches long in the flow direction. The charcoal filter is a Barneby Cheney Model PAB type filter, 8 x 8 x 1-1/8 inches in outside dimensions, with Type AC activated charcoal, 6 to 10 Tyler mesh size. The charcoal filter is rated for an airflow of 20 cfm (NTP) and a pressure drop of 0.3 inch water.

The actual pressure drop through both filters during electrolysis-cell operation was measured as 1.0 inch water at a total airflow of 21.8 cfm (NTP), which corresponds to a superficial air velocity of 0.82 fps through an 8 x 8-inch face area.

Contaminant-Injection Studies

Introduction

The objective of the contaminant-injection experiments was to study the effect of electrolysis-cell operation (anodic oxidation, ozone) on typical atmospheric contaminants, such as carbon monoxide, methane, and airborne microorganisms. The study was carried out by injecting a known amount of a selected contaminant into the anodic side of the box enclosing the electrolysis unit and determining how rapidly the injected contaminant disappears in the box. Since the injected contaminant was entrained out of the box by the outflow of the anodic gas, this mode of contaminant removal from the box must be differentiated from that brought about by electrolysis-cell operation.

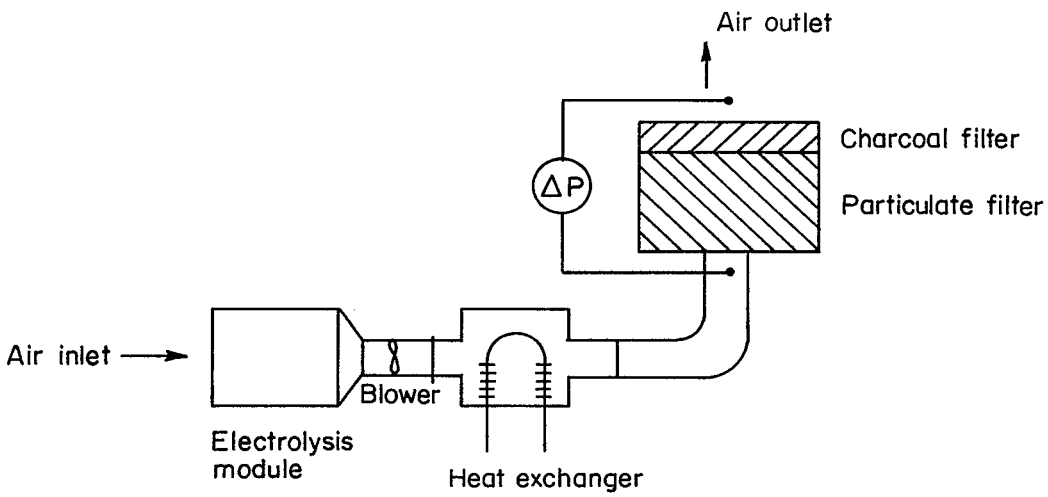

FIGURE 5. SCHEMATIC OF CHARCOAL FILTER AND PARTICULATE FILTER ASSEMBLY

To estimate the entrainment rate, the following material-balance equation may be used:

$$V \frac{dc}{dt} = - vc \quad . \tag{5}$$

Integration of Equation (5) between the limits, $c = c_i$ at $t = 0$ and $c = c$ at $t = t$ yields the following relationship, which expresses the decay of the contaminant level in the box due to entrainment:

$$\frac{c}{c_i} = \exp \left(\frac{-vt}{V} \right) \quad . \tag{6}$$

Solution of Equation (6) for $v = 1.59$ ft^3/hr and $V = 2.5$ ft^3 yields the results shown below:

t, hr	c/c_i
0	1
0.1	0.938
0.5	0.727
1.0	0.472

The results indicate that 27.3 percent of the contaminant injected would be lost by entrainment in 0.5 hour after injection, which gives sufficient time to obtain samples for analysis.

Gaseous Contaminants

Hydrogen, originally selected together with carbon monoxide and methane for the experiment, was deleted from the experiment because of the cell cross-leakage problem. Helium was injected simultaneously with carbon monoxide and methane to serve as a reference for direct comparison.

Gas samples were taken directly from the box at intervals of 5, 15, 30, and 60 minutes after injection and analyzed by gas chromatography.

Airborne Microorganisms

One milliter of an overnight culture of the bacteria [Bacillus Subtilis var. Niger (globigii)] was inoculated into 100 ml of nutrient broth (Difco) and incubated at 37 C on a reciprocating shake machine for approximately 8 to 12 hours. The culture was harvested by centrifugation at 17,000 x g for 20 minutes and resuspended in M/15 phosphate buffer (pH 7.0). The organisms were injected into the electrolysis-cell box from the phosphate buffered bacterial suspension with a No. 40 DeVilbiss (The DeVilbiss Company, Toledo, Ohio) all-glass atomizer. Samples of the gaseous environment containing the bacteria inside the electrolysis-cell box were obtained with a critical orifice liquid impinger[9] containing 20 ml of a dilute gelatin solution (2.0 g gelatin/1 M/15 phosphate buffer, pH 7.0). The sampling time was approximately 3.0 seconds, and the average volume of gas samples was about 620 ml. The dilute gelatin solutions were diluted serially by 10 in phosphate buffer (pH 7.0) and each dilution plated in duplicate on standard-plate-count agar (Difco). All of the plates were incubated at 37 C for 72 hours.

EXPERIMENTAL RESULTS

Operation of Electrolysis Unit

For the trace-contaminant studies, the electrolysis unit was operated with the 12 cells connected in the parallel/series configuration. During operation, measurements were taken on cell operating variables that included module voltages, module current, air temperature and humidity at the inlet of the module, air-temperature increase between the inlet and the outlet of the module, and the rate of hydrogen production. Steady-state operating conditions of the electrolysis unit during the entire period of trace-contaminant studies are summarized in Table 1.

TABLE 1. STEADY-STATE OPERATING CONDITIONS OF ELECTROLYSIS UNIT WITH CELLS CONNECTED IN PARALLEL/SERIES CONFIGURATION

	Operating Mode			
	Normal		Off-Normal	
	Without Filters	With Filters	Without Filters	With Filters
Total Operating Time, hr	397	87	97	74
Air Temperature at Module Inlet, F	75.0 ± 0.5	75.0 ± 0.5	75.0 ± 0.5	75.0 ± 0.5
Relative Humidity at Module Inlet, percent	50 ± 2	50 ± 2	50 ± 2	50 ± 2
Air-Temperature Increase Through Module, F	5 ± 1(a)	5 ± 1(a)	7 ± 1(a)	7 ± 1(a)
Airflow Parameter (n), dimensionless	30 ± 6	30 ± 4	22 ± 3	22 ± 3
Module Current, amperes	10.7	11.4	13.0	13.0
Module Voltage, volts	6.41	6.46	6.60	6.61
Typical Cell Group Voltage, volts				
Group 1	2.171	2.184	2.235	2.251
Group 2	2.140	2.141	2.185	2.183
Group 3	2.099	2.132	2.180	2.176
Hydrogen Collection Efficiency, percent	100 ± 1	100 ± 1	100 ± 1	100 ± 1
Hydrogen Production, cm^3/min (STP)	223	238	272	272
Oxygen Production, cm^3/min (STP)	112	119	136	136

(a) Deviation indicated refers to fluctuation rather than measurement accuracy which was ±0.1 F.

The electrolysis unit was operated under both normal and off-normal conditions and also with and without the charcoal filter and the particulate filter in line. As shown in Table 1, for the nominal design conditions of 75 F and 50 percent relative humidity, the rated capacity of the module (1/4-man, 10.6 amperes, 110 cm^3 O_2/min, STP) could be maintained in the normal operating mode of 6.45 volts or less.

After the trace-contaminant studies were completed, the electrolysis unit was rewired to connect the 12 cells in the series configuration to study the voltage characteristics of the individual cells. The electrolysis unit was then operated at two different

TABLE 2. STEADY-STATE OPERATING CONDITIONS OF ELECTROLYSIS/UNIT WITH CELLS CONNECTED IN SERIES CONFIGURATION

	Relative Humidity at Module Inlet, percent	
	48 ± 2	40 ± 2
Total Operating Time, hr	55	54
Air Temperature at Module Inlet, F	75.0 ± 0.5	75.0 ± 0.5
Air-Temperature Increase Through Module, F	5.2 ± 0.5	4.0 ± 0.5
Airflow Parameter (n), dimensionless	26 ± 4	30 ± 4
Module Current, amperes	2.65	1.95
Cell Current Density, amp/ft^2	34.7	25.5
Module Voltage, volts	25.45	25.54
Typical Cell Voltage, volts		
Cell 1	2.172	2.182
Cell 2	2.105	2.105
Cell 3	2.146	2.125
Cell 4	2.164	(a)
Cell 5	(a)	(a)
Cell 6	2.118	2.106
Cell 7	2.061	2.080
Cell 8	2.148	2.146
Cell 9	2.082	2.069
Cell 10	2.200	2.205
Cell 11	2.099	2.086
Cell 12	2.141	2.113
Hydrogen collection efficiency, percent	100 ± 1	100 ± 1
Hydrogen Production, cm^3/min (STP)	221	
Oxygen Production, cm^3/min (STP)	111	

(a) A poor voltage-lead connection prevented obtaining voltage on Cells 4 and 5.

relative humidities, 48 percent and 40 percent, at the module inlet. The unit was operated under normal conditions of average voltage of about 2.15 volts/cell without the filters in line. Steady-state operating conditions for the electrolysis unit are summarized in Table 2. Further details on cell voltage characteristics are contained in Appendix B.

During the experimental studies at Battelle the ARC module was operated satisfactorily for over 1000 hours (45 days) during an 85-day period and was in satisfactory working condition when returned to Ames Research Center for further evaluation. The total accumulated operating time of 145 days (3500 hours) on the ARC module without evidence of deterioration in performance at the nominal design operating conditions represents a significant advance in the state of the art of water electrolysis cells with respect to operational reliability.

Ozone Production and Control

Table 3 summarizes the results of measurement of ozone generation rates. The significant increase in ozone production with increase in voltage for off-normal operation was consistent with prior results reported for sulfuric acid electrolyte.[3]

TABLE 3. CONCENTRATIONS OF OZONE AND ACID SPRAYS WITH AND WITHOUT CHARCOAL AND PARTICULATE FILTERS

Electrolysis-Unit Operating Conditions	Ozone, ppm based on oxygen	
	Without Charcoal Filter	With Charcoal Filter
Normal (6.45 volts)	0.11	0.0025
Off-normal (6.60 volts)	5.0	0.0025
	Sulfuric acid, ppm based on oxygen	
	Without Particulate Filter	With Particulate Filter
Normal (6.45 volts)	1.1	<0.00001
Off-normal (6.60 volts)	1.4	<0.00001

The effectiveness of the charcoal filter in reducing the ozone concentration to at least the limit of detection of 0.0025 ppm is shown by the data in Table 3. Probably higher ozone production rates could have been controlled. Presumably, ozone is adsorbed on the charcoal and subsequently decomposes to oxygen; thus it would not affect the life of the charcoal filter. The experimental results are significant in that they indicate that charcoal filters as normally used to treat cabin air would control ozone produced by the electrolysis cell at a level about 10 times lower than the 90-day limit of 0.02 ppm for spacecraft.

Acid-Spray Production and Control

The concentration of sulfuric acid spray contaminant in the oxygen shown in Table 3 was about the same as that estimated from prior studies of water-vapor electrolysis cells (with phosphoric acid electrolyte). The percentage of the electrolyte lost as acid spray is negligible (1 ppm corresponds to a loss of about 0.1 gram/year from a 1-man electrolysis unit containing about 500 grams of electrolyte). The particulate filter was effective in reducing the acid spray to the limit of detection and well below the assumed 90-day spacecraft limit of 0.1 ppm. As with ozone, the experimental results are significant in that they indicate the effectiveness for control of acid by the type of particulate filter normally used in space cabin simulators for filtering cabin air.

Identification of Contaminants Other than Ozone and Acid Sprays

The electrolysis unit was operated under normal conditions without the charcoal and the particulate filters in line, and also under off-normal conditions with and without the filters in line. Operating conditions of the electrolysis unit are given in Table 1.

Experimental results obtained during normal electrolysis-cell operation without the filters are summarized in Table 4. Small quantities of hydrogen were found in the oxygen sample, indicating a cell cross-leakage. Oxygen and nitrogen found in the hydrogen sample could have originated from the cell cross-leakage or the ambient air trapped in the sampling line. The oxygen sample showed very few contaminants except for some carbon dioxide. All compounds identified in the analysis are present in quantities well below the 90-day limits for spacecraft. Trace quantities of hydrocarbon compounds found in the hydrogen sample are probably insignificant as far as the purity of the hydrogen for use in carbon dioxide reduction is concerned. No sulfur compounds were detected in the hydrogen.

Experimental results obtained during off-normal operation of the electrolysis unit with and without the charcoal and the particulate filters in line are shown in Table 5. The results are similar to those obtained during normal operation of the electrolysis unit. Acetylene was detected in the sample obtained with the filters in line. Most likely it came from the cylinder nitrogen used in this particular run, as indicated by an analysis of the cylinder nitrogen. The anodic gas obtained with the filters in line contained 100 to 200 ppm of carbon dioxide, which is about an order of magnitude higher than the concentrations found in other samples. Possibly, the carbon dioxide was adsorbed on the charcoal filter from room air prior to use in the experiment. There is no practical significance to the presence of carbon dioxide in the range of 100 ppm (0.01 percent) from the standpoint of either toxicity or an added penalty for its removal in the life-support system aboard spacecraft.

It may be concluded from the experimental results obtained that no trace contaminant of concern to production of breathing oxygen is generated from operation of the water-vapor electrolysis unit under the operating conditions investigated.

TABLE 4. ANALYSIS OF GASES DURING NORMAL OPERATION WITHOUT FILTERS IN LINE

Sample	Compound Analyzed										
	Mole Percent			Parts per Million							
	O_2	N_2	H_2	CO_2	HCl	C_3-HC[a]	C_2H_6	C_2H_4	SO_2	H_2S	COS
Oxygen	17.6	82.1	0.26	6	<0.01	0.01	<0.01	<0.01	<0.01	<0.01	<0.01
	17.2	82.7	0.07	6	<0.01	<0.01	<0.01	<0.01	<0.01	<0.01	<0.01
Hydrogen	0.05	0.19	99.8	0.9	<0.01	0.05	0.4	<0.01	<0.01	<0.01	<0.01
	0.04	0.18	99.8	1	<0.01	0.03	0.3	<0.01	<0.01	<0.01	<0.01

(a) Unidentified C_3 hydrocarbon.

TABLE 5. ANALYSIS OF GASES DURING OFF-NORMAL OPERATION WITH AND WITHOUT FILTERS IN LINE

Sample	Compounds Analyzed											
	Mole Percent			Parts per Million								
	O_2	N_2	H_2	CO_2	HC_1	C_3-HC[a]	C_2H_6	C_2H_4	C_2H_2	SO_2	H_2S	COS
Without Filters												
Oxygen	25.3	74.5	0.12	11	<0.01	0.02	0.07	<0.01	–	<0.01	<0.01	<0.01
	25.4	74.4	0.16	10	<0.01	0.03	0.07	<0.01	–	<0.01	<0.01	<0.01
Hydrogen	0.08	0.32	99.6	1	<0.01	0.05	0.30	<0.01	–	<0.01	<0.01	<0.01
	0.04	0.24	99.7	1	<0.01	0.07	0.46	<0.01	–	<0.01	<0.01	<0.01
With Filters[b]												
Oxygen	19.7	80.2	0.05	200	<0.01	0.05	<0.01	<0.01	0.19	<0.01	<0.01	<0.01
	20.0	79.9	0.05	100	<0.01	0.04	<0.01	<0.01	0.10	<0.01	<0.01	<0.01

(a) Unidentified C_3 hydrocarbons.

(b) The cylinder nitrogen used for this run contained 0.03 ppm argon, 0.54 ppm oxygen, 16 ppm CO_2, 0.09 ppm C_2H_6, 0.1 ppm CH_3OH, and 5 ppm C_2H_2.

TABLE 6. GAS-INJECTION STUDIES

Gas Injected	Time After Injection, minutes	Concentration, ppm Measured	Concentration, ppm Calculated[a]	Concentration Measured / Calculated Concentration
CO	0	--	113	--
	5	84	107	0.78
	15	79	96	0.82
	30	65	82	0.79
	60	62	60	1.03
			Average	0.86
CH_4	0	--	113	--
	5	82	107	0.77
	15	75	96	0.78
	30	58	82	0.71
	60	52	60	0.87
			Average	0.78
He	0	--	150	--
	5	114	142	0.80
	15	106	128	0.83
	30	92	109	0.84
	60	76	79	0.96
			Average	0.86

(a) Calculated values were obtained from the following equation:

$$\frac{c}{c_o} = \exp\left(\frac{-vt}{V}\right) ,$$

where

c_o = Initial concentration
v = Total gas output from the anodic side, 0.0265 cfm
V = Total gas volume on anodic side, 2.5 ft^3
t = Time after injection, min.

TABLE 7. THE EFFECT OF THE GASEOUS ENVIRONMENT IN A SULFURIC ACID-WATER VAPOR ELECTROLYSIS CELL ON THE SURVIVAL OF BACILLUS SUBTILIS VAR. NIGER

Exposure Time, min	Number of Viable B. Subtilis var. Niger Cells per 620 Ml of Air Sampled
2.5	7200
10	400
20	100
30	0
40	0
50	100
60	100
120	0
180	0

Injection of Gaseous Contaminants

The experiment was carried out by injecting a known amount of gases into the anodic side of the electrolysis unit and determining the decay of the injected gases inside the box. The electrolysis unit was operated under normal conditions without the filters in line. Operating conditions for the electrolysis unit during the experiment are given in Table 1.

Experimental results are given in Table 6. The calculated values of the concentrations (in ppm) were consistently higher than the measured values. The deviations between the calculated and the measured concentrations were about the same between the test gases (carbon monoxide and methane) and the reference gas (helium). This indicates that the test gases decayed at about the same rate as the inert reference gas. Therefore, it may be concluded that carbon monoxide and methane were not removed by reaction(s) on the anodic surface of the water-vapor electrolysis cell under the experimental conditions used.

Injection of Airborne Microorganisms

The objective of this task was to investigate the effect of electrolysis-cell operation on airborne microorganisms. The study was performed by injecting a test organism into the air on the anodic side of the electrolysis unit and determining the decay of the bacterial count. The test organism used in the experiment was a laboratory culture of Bacillus subtilis var. niger (globigii). The electrolysis unit was operated under normal conditions without the filters in line. Operating conditions for the electrolysis unit during the experiment are given in Table 1.

The results of the gas-sampling experiment are presented in Table 7. It is readily apparent that a sudden decrease in the number of viable cells of the bacteria occurred during the first 10 minutes of exposure to the environment inside the electrolysis-cell box. Very few viable organisms could be detected after the 10-minute sample. Although the results represent only one experiment, there is a strong indication that the organisms are destroyed rapidly by the electrolysis-cell operation.

CONCLUSIONS

On the basis of the results obtained from the trace-contaminant studies, the following conclusions may be drawn:

(1) Major contaminants generated from operation of a sulfuric acid water-vapor electrolysis unit are ozone and acid-electrolyte sprays. Under normal operating conditions at a nominal module voltage of 6.45 volts, the concentrations of the ozone and acid sprays are 0.11 ppm and 1.1 ppm, respectively, based on oxygen produced. These concentrations exceed the 90-day limits for spacecraft. Under off-normal operating conditions at a nominal module voltage of 6.60 volts, the ozone and the acid-spray concentrations increase to 5.0 ppm and 1.4 ppm, respectively, based on oxygen produced.

(2) The ozone and the acid sprays generated from water-vapor electrolysis can be removed efficiently by an activated-charcoal filter and a fiberglass-type particulate filter. With the filters in line, the ozone and the acid-spray concentrations are reduced to 0.0025 ppm and less than 0.00001 ppm, respectively, based on oxygen produced under both normal and off-normal operating conditions. These concentrations are below the 90-day limits for spacecraft.

(3) Besides ozone and acid sprays, no other contaminant of practical significance is generated from operation of the water-vapor electrolysis unit.

(4) There is little indication that carbon monoxide and methane at levels below 200 ppm on the anodic side of the electrolysis unit are removed by reaction(s) on the anodic surface.

(5) There is a strong indication that airborne microorganisms are rapidly destroyed on the anodic side of the water-vapor electrolysis unit.

SECTION 3. SYSTEM INTEGRATION ANALYSIS

SCOPE OF STUDY

For purposes of this study, the "water-vapor electrolysis cell" is considered a design concept that can be distinguished from other water electrolysis cells being developed by the following definition:

> An electrolysis cell with acid electrolyte that operates by simultaneous oxygen generation and water-vapor absorption at the anode with a carrier gas moving across the anode by forced convection to provide cell cooling and with hydrogen gas generation at the cathode.

The above definition is sufficiently broad to include any acid electrolyte (e.g., sulfuric acid or phosphoric acid); any source of water vapor (e.g., water vapor in cabin air or water vapor recovered from another subsystem); and open-loop operation (e.g., concurrent dehumidification, with cabin air as carrier gas and anode at cabin pressure) or closed-loop operation (e.g., oxygen carrier gas and anode at pressure above cabin pressure).

As defined above, the water-vapor electrolysis cell is quite versatile and should perform the primary function of electrolytic oxygen production over a wide range of possible design specifications. The design specifications for a prototype electrolysis unit will depend on:

(1) Integration factors (i.e., the other subsystems in the overall life-support system)

(2) Interface considerations involving interaction with other specific subsystems in a direct manner (i.e., hydrogen delivery pressure, partial pressure of water vapor supplied to electrolysis unit, voltage regulation of power supply) or an indirect manner (i.e., atmosphere contaminant control, thermal control, and humidity control).

From a consideration of integration and interfacing, it is expected that approximate quantitative values can be established for design specifications. Only then can specific prototype designs be considered and specific choices be made with respect to possible design features, for example, the choice between various operating parameters (i.e., high or low current density) and the choice between various methods of operational control.

As a result of this analysis, it is expected that a priority of research needs can be established. Top priority is directed toward factors that would influence the design of a prototype unit (i.e., 4-man unit) in the near future. A basis for design specifications is an electrolysis unit that could be evaluated in a manned chamber [e.g., Integrated Life Support System (ILSS) at NASA Langley Research Center[8]].

DISCUSSION OF HYDROGEN-DELIVERY-PRESSURE SPECIFICATION

One interface problem relating to the water-vapor electrolysis cell depends on the hydrogen-delivery-pressure specification which in turn depends on how the hydrogen is to be used in an integrated life-support system. The problem can be analyzed by considering the two possible cases:

Case I. The hydrogen is not needed and is vented overboard.
Case II. The hydrogen is to be used in a partially closed life-support system.

Venting Hydrogen to Space Vacuum

There does not appear to be any particular problem for Case I that could not be resolved by suitable cell design and pressure relief controls to vent hydrogen to space vacuum. At the present time, there is no cell design problem when only a small differential pressure exists across the matrix between the hydrogen gas and the atmosphere on the anode side (i.e., air or oxygen). For example, Module 2 was operated at Battelle-Columbus for 1700 hours with practically stoichiometric collection of hydrogen (100 ± 1 percent) with the hydrogen rate measured by a wet test meter at a slight positive pressure of 1 to 2 inches of water.[4] When the back pressure on the hydrogen was increased above 6 inches of water, some hydrogen leakage occurred at the external porting connections. While minor improvement in cell design with regard to hydrogen porting is needed, the present evidence shows that no immediate problem should exist for maintaining a small differential pressure while venting hydrogen to space vacuum with a suitable pressure relief valve. Probably, the pressure relief valve would be referenced to the cabin pressure to maintain the required small positive differential pressure between hydrogen and cabin air for open-loop operations. Such a control system would be designed for automatic control over a range of cabin pressures from 5 psia to 14.7 psia. A similar control system would be used for closed-loop operation with the pressure relief valve for venting hydrogen to space vacuum referenced to the pressure of the oxygen recirculated in the loop.

For open-loop operation of the water-vapor electrolysis cell, the question has been raised of cell operation during emergency decompression of the cabin. It would be important to maintain the hydrogen differential pressure within prescribed limits by venting hydrogen as the cabin pressure decreased. This should be no problem for the automatic controls suggested above provided the cabin pressure decreased relatively slowly. For example, it has been estimated, with reference to the AILSS cabin volume of 10,000 ft^3, that for a 1-inch-diameter hole it would take 1 hour for the cabin pressure to be reduced to 2 psia. It is expected that other controls for the electrolysis cell would shut down electrolysis-cell operation when the cabin pressure fell below a prescribed minimum (i.e., if forced air circulation was insufficient to prevent cell overheating).

Interfacing With CO_2 Reduction System

The interfacing of the water-vapor electrolysis cell is primarily concerned with the hydrogenation systems (Sabatier and Bosch). There is no way that the hydrogen from water electrolysis can be utilized in either the "molten carbonate system" or "solid electrolyte system" for oxygen recovery from carbon dioxide. Thus, the problem of hydrogen delivery pressure is an interface problem with the Sabatier or Bosch system in the many variations of these systems. Other uses for hydrogen than reaction with carbon dioxide in a closed atmosphere-control system are outside the scope of the present analysis.

The problem of hydrogen delivery pressure for Case II can be considered relative to the possible modes of operation of the water-vapor electrolysis cell:

Case IIA. Closed-Loop Operation
Case IIB. Modified Open-Loop Operation
Case IIC. Open-Loop Operation.

Closed-Loop Operation

For closed-loop operation there does not appear to be a problem relative to hydrogen pressure, because the recirculating loop can be designed for the absolute pressures needed and a small differential pressure between hydrogen and oxygen can be maintained. The closed-loop system can be designed to operate relatively independent of cabin-pressure changes including decompression. Furthermore, the temperature and humidity of the gas feed to the water-vapor electrolysis cell can be preselected and controlled to favor operation of it. Thus, many advantages are seen for closed-loop operation compared with open-loop operation. The main advantage of open-loop operation relates to dehumidification, and the advantages relating to dehumidification must be considered relative to the possible problem of hydrogen delivery pressure for open-loop operation.

Modified Open-Loop Operation

Before discussing open-loop operation, it is well to point out that there is the possibility of retaining some of the advantages of open-loop operation and closed-loop operation in a system that could be called "modified open loop" operation. In the latter system, a circulating loop is operated at an elevated pressure (above cabin pressure) selected so as to provide the hydrogen at the required delivery pressure with a small differential pressure across the cell matrix. Partial dehumidification of cabin air would be accomplished by providing a compressor to increase a portion of the cabin air to a pressure for feed to the circulating loop. Thus, the water vapor can be removed from the cabin air by the electrolysis cell in the loop and oxygen-enriched air from the loop is vented back to the cabin. The added equipment needs for the "modified open loop" compared to those for open-loop operation are the loop structure, circulation blower, and the air compressor. The added components indirectly permit hydrogen delivery at pressures required for the Sabatier or Bosch reactor based on demonstrated capabilities of the water-vapor electrolysis cell. Further analysis of the pros and cons of "modified open-loop" operation will be considered in future work.

- Open-Loop Operation

The hydrogen delivery pressure required for feed to the Sabatier or Bosch is not known exactly. It can be assumed that the pressure will not be higher than 20 psig relative to cabin pressure, and it might be lower. For most water electrolysis cells there is no appreciable concern for hydrogen delivery pressure since the water-feed cells are usually operated as closed systems with water feed at the required pressure. The need for additional controls and sturdy structure is usually accepted. An analogy can be made to the closed-loop operation of the water-vapor electrolysis cell. Because of this, it has been common in the past to specify that hydrogen (and oxygen) from electrolysis be provided at a sufficiently high pressure (i.e., 20 psig) that there would be no problem in hydrogen feed to the Sabatier or Bosch reactor. The hydrogen-pressure specification is probably conservatively on the high side. Only for open-loop operation of the water-vapor electrolysis cell on air at reduced cabin pressure is the hydrogen delivery pressure of concern. There is a need to review the basis for a hydrogen-pressure specification with regard to the specific subsystem interface (Sabatier or Bosch) and the possible penalty for open-loop operation of the electrolysis cell.

Significance of Hydrogen-Pressure Specification for Cell Design

The specification for hydrogen delivery pressure is of concern in water-vapor electrolysis cell design and operation for the following reasons:

(1) A significant increase in hydrogen pressure (i.e., above about 0.5 psi) relative to cabin pressure would require a sturdy cell construction with regard to the cathode sections of the module and more positive sealing of hydrogen. Thus, the cell weight would be increased as the hydrogen-pressure specification is increased.

(2) As the hydrogen-pressure specification is increased, the requirements of the matrix are increased with regard to "bubble pressure" (i.e., the pressure at which hydrogen crossleak would occur through the largest pore of the porous matrix). A matrix with adequate "bubble pressure" (above 20 psi) is possible. Certain asbestos matrices developed for fuel cells are reported to have "bubble pressures" of 50 to 150 psi. However, at the present time no data are available on "bubble pressure" for the matrices that have been used in the water-vapor electrolysis cell design (neither the silica gel/microporous PVC matrix used at NASA Ames nor the asbestos/microporous rubber matrix used at Battelle-Columbus). Such data should be obtained in the future. A standard matrix bubble pressure is usually determined by independent evaluation of the matrix apart from the physical design of the cell with regard to edge sealing and porting.

(3) Standard matrix "bubble pressure" (as usually independently determined apart from the cell) is predicated on a degree of liquid saturation of the matrix to fill all the interconnecting pores of the matrix. However, in practice the volume of electrolyte in the matrix can change during cell operation as the concentration of the electrolyte changes. The electrolyte concentration automatically adjusts to the variables of humidity, temperature, and current density for the imposed conditions of voltage and air flow. Thus, "bubble pressure" is related to the range of cabin-air variables that the cell can tolerate and to the auxiliary controls needed for cell operation. For example, if the cell matrix tends to "dry out" (i.e., electrolyte concentration increases and volume of electrolyte decreases) there may be insufficient electrolyte to fill all the pores, and the

effective bubble pressure is reduced. Whether or not crossleak of hydrogen to the air stream occurs depends on whether the differential pressure across the matrix (based on hydrogen-pressure specification) is less than the effective bubble pressure under all cell operating conditions that are permitted. Thus, hydrogen-pressure specification indirectly influences the operational limits of the water-vapor electrolysis cell operating on cabin air and might define the need for operational controls. It is apparent that matrix design (materials, porosity, and thickness) influences both standard bubble pressure and effective bubble pressure, or the effect of electrolyte-volume changes on degree of matrix saturation. Thus, whether a particular matrix design is satisfactory to prevent crossleak of gas is a complex question, and obtaining a definitive answer would involve considerable experimental study. Therefore, analytical studies providing a better understanding of cell operation based on equations for heat and mass transfer are important to minimize the work of experimental verification.

(4) In addition to "drying out" of the matrix and crossleak of hydrogen discussed in (3) above, the alternative problem of overdilution of the matrix is equally important. While gross flooding and loss of electrolyte is not expected to be a problem except under extreme abnormal operating conditions, overdilution is known to contribute to increase of "acid spray" and the trace-contaminant problem. The hydrogen-pressure specification could be important to the acid-trace-contaminant problem for two reasons:

(a) There are restrictions on overdesign towards a "wet matrix" so as to counteract the problems related to bubble pressure and hydrogen pressure. (Note that this problem is unique to an electrolysis cell generating oxygen as opposed to fuel cells for which extensive studies relating to bubble pressure are available.)

(b) It is expected that an increase in hydrogen pressure would tend to force electrolyte away from the cathode screen and towards the anode screen. The use of a matrix of small pore size relative to the electrodes tends to minimize the problem. However, empirical knowledge that has been the guide to the proper initial impregnation of the matrix with acid for operation at low differential pressure might not be adequate if the hydrogen-pressure specification is increased (i.e., adequate knowledge to avoid an increase in acid spray contamination). Thus, the evaluation of a cell matrix design and initial acid impregnation with respect to hydrogen pressure would be incomplete without simultaneous evaluation of trace contaminants (acid and hydrogen in air stream) and current/voltage performance.

Hydrogen-Delivery-Pressure Requirements

Bosch System

Information on the minimum hydrogen-delivery-pressure requirements for feed to the Sabatier or Bosch reactor is not readily available, because most studies of hydrogenation systems were predicated on the availability of hydrogen at pressure without any significant penalty to the water electrolysis system. For example, recently completed studies[11] of the Bosch system at Battelle-Columbus were originally based on integration with a water-vapor electrolysis cell using Pd-25Ag cathodes operating in a closed loop. Experimental data had shown that with Pd-25Ag cathodes, hydrogen could be delivered at 20 psig with the closed design for operation at atmospheric pressure.

Later substitution of the water-vapor electrolysis cell with acid electrolyte[4] into the latter integrated system served the purpose of evaluating the water-vapor transfer subsystem. However, evaluation of the hydrogen-interface problem was not possible with the available equipment. As originally designed and operated, the Bosch system would have required a minimum delivery pressure of hydrogen of 3 psig at the inlet to the Bosch recycle pump. The available acid-type electrolysis unit (Module 2) was limited to about 6-inch H_2O differential pressure, and the closed-loop water-vapor transfer system had not been designed for operation at positive pressures (i.e., 3 psig for oxygen recirculated in the loop). Thus, no attempt was made to use the hydrogen produced by the water-vapor electrolysis cell for feed to the Bosch reactor.

A recent preliminary analysis of the operation of the Bosch system available at Battelle-Columbus indicates that it could be modified so that the inlet pressure to the recycle pump could be maintained at atmospheric pressure (i.e., cabin pressure) or slightly less so as to accept hydrogen feed from the water-vapor electrolysis cell operating on room air (i.e., cabin air). The Bosch-system pressure and reaction rate would be controlled by carbon dioxide feed. Present systems of carbon dioxide concentration (i.e., regenerable adsorbers) include accumulators so that carbon dioxide is available at pressures for feed to the Bosch reactor.

The Bosch reaction is not particularly sensitive to pressure. Therefore, the choice of operating pressure might be related to any gas leakage problems which must be considered for high-temperature reactors. Assuming that the pressure drop across the recycle pump (through the Bosch reactor) is 2 psi, one might design for ambient pressure ±1 psi. There is concern for leakage of air into the Bosch system and also concern for leakage of Bosch reaction gases containing 20 to 60 percent carbon monoxide out of the system to the cabin. Perhaps the latter is the more important consideration, in view of the low limits on atmospheric contamination with carbon monoxide (15 ppm). Thus, it might be desirable that the Bosch system be designed so that nowhere in the Bosch recycle loop does the pressure exceed ambient. It is also possible that future designs of the Bosch system would consider a partial vacuum jacket around the hot portions of the equipment to reduce heat losses and contain any leakage gases which could be easily purged to space vacuum. For the latter approach, it would also be desirable to design the Bosch system for operation at low absolute pressure (e.g., 2 to 5 psia).

In summary, a preliminary analysis of the Bosch system indicates that there is no apparent reason why the hydrogen feed to the Bosch has to be at high pressure. The Bosch system could be designed for operation at all times at or below cabin ambient pressure, which would be compatible with the water-vapor electrolysis cell operating on ambient cabin air with the hydrogen available at only a slight positive pressure.

Sabatier System

Possibly, the earliest integration of a prototype water-vapor electrolysis unit in a life-support system will involve interfacing with an open Sabatier system. The minimum hydrogen-feed-pressure requirements for the conventional Sabatier system are not easily defined at the present time. In general, the Sabatier units that have been developed have been designed for hydrogen feed at elevated pressure. At the present state of the art, the main interest has been in the open Sabatier system coupled with a regenerable adsorbent CO_2 concentrator (silica gel/molecular sieve), and utilization of hydrogen

from water electrolysis. Some further discussion of the Sabatier system will indicate the immediate difficulty in defining hydrogen-feed-pressure requirements.

The Sabatier reaction is: $CO_2 + 4H_2 = CH_4 + 2H_2O$. The open Sabatier system is a one-pass system with the methane dumped overboard along with any unreacted hydrogen or CO_2 after water has been recovered. (The closed Sabatier system refers to recovery of hydrogen from methane for further reaction with available carbon dioxide to maximize water recovery). In one variation of the open Sabatier, makeup hydrogen is supplied from stores to utilize all of the carbon dioxide. The Sabatier is operated hydrogen-rich with an excess of hydrogen above the stoichiometric ratio of 4:1. The excess hydrogen is required for high percentage conversion of CO_2 to CH_4 and some hydrogen is usually lost with the methane. It is debatable whether carrying extra hydrogen on board offers a favorable weight trade-off.

A second variation of the open Sabatier does not involve stored supplies, and only available hydrogen from electrolysis is used and the excess CO_2 is discarded. Vacuum purging of CO_2 from molecular sieves for regeneration will be used on early missions because of the low power requirement. Compared to vacuum purging for regeneration, recovery of CO_2 in concentrated form for feed to the Sabatier reactor involves an added penalty for regeneration (waste heat and/or electrical power plus accumulators). Thus, it would appear desirable to collect only the CO_2 that could be used in the open Sabatier reaction and purge the excess CO_2 from the adsorbent directly to space vacuum. With the Sabatier operated in the hydrogen-rich mode, some hydrogen is lost with the methane.

A third variation involves recovery of all CO_2 and operation of the Sabatier reaction in the CO_2-rich mode to maximize utilization of available hydrogen, and thus maximize water recovery. Excess unreacted CO_2 is dumped overboard with the methane. The trade-off involves the credit for additional water recovered by efficient utilization of hydrogen versus the penalty for concentrating all of the CO_2. The trade-off would favor operating the Sabatier CO_2-rich when the open Sabatier is considered as a backup mode of operation to the Bosch system (i.e., ILSS at NASA Langley).[8] Since the system design for Bosch operation requires collection and concentration of all of the CO_2, the CO_2 is available for operation CO_2-rich in the alternative mode of open Sabatier.

In considering the hydrogen-pressure requirements of the Sabatier system, it appears necessary to make a distinction between the two modes of operation: hydrogen-rich and CO_2-rich.

For the hydrogen-rich mode of operation, hydrogen feed pressure is important for two reasons:

(1) Theoretical considerations of the Sabatier reaction indicate that high pressure favors high percentage conversion of CO_2 to CH_4 (i.e., 5 moles of reactants yield 3 moles of products). High conversion minimizes the amount of hydrogen dumped overboard with methane.

(2) The Sabatier reaction, being a one-pass system, is more sensitive to feed ratio of hydrogen to CO_2 than is the Bosch reaction. Thus, careful control of hydrogen feed rate might be important, and gas-feed control devices can cause pressure drops. Also, to even out possible fluctuations in hydrogen generation rate, it might be desirable to use a small hydrogen accumulator which would also require hydrogen generation at pressure. A detailed trade-off analysis would be required to determine the optimum

combination of water-vapor electrolysis cell hydrogen delivery pressure and Sabatier operating pressure considering pumps, accumulators, and controls for hydrogen-rich operation of the Sabatier.

While there has been much experimental work reported on hydrogen-rich operation of the Sabatier, there are relatively few published data on the more recent trend toward CO_2-rich operation of the Sabatier. In general, there is negligible carbon monoxide formation in hydrogen-rich operation of the Sabatier. It is not known whether this is true for CO_2-rich operation or whether the presence of carbon monoxide in the product gases of the Sabatier is a significant factor. The possibility of leakage of gases containing carbon monoxide should not be any greater concern than in the case of the Bosch or solid electrolyte system. However, it was of interest to learn that in the recent 60-day manned chamber run at Douglas, the Sabatier reactor was operated at cabin pressure even though both hydrogen and CO_2 were available at high pressure (above 20 psig). Operation of the Sabatier at cabin pressure (10 psia) probably provided a greater margin of safety for the first use of the Sabatier in an extended manned run. Also, the Sabatier was operated CO_2-rich during part of the run. Technical data on performance of the Sabatier in the 60-day run have not been available as yet.

Possible Methods of Providing Hydrogen Pressure for Open-Loop Operation

The experimental data available at the present time on operation of water-vapor electrolysis cells are insufficient to define whether a problem exists in providing hydrogen under pressure for open-loop operation. However, no insurmountable technical problem is foreseen. The question requiring further study is which of several approaches would provide the best overall system for open-loop operation. The possible solutions are discussed below:

(1) With a conventional pump or compressor as part of the water-vapor electrolysis cell system, the inlet pressure to the pump would be controlled to provide a small positive differential pressure of hydrogen relative to cabin pressure (it is assumed that crossleak of oxygen or air into the hydrogen is less desirable than crossleak of hydrogen into the air or oxygen). The pump would deliver hydrogen at the required discharge pressure for direct feed to the Sabatier or Bosch. Possibly a small-volume hydrogen accumulator in the line after the pump discharge would be desirable. Obviously, the requirement for a pump (and possibly the accumulator) would penalize the water-vapor electrolysis system in any tradeoff versus other approaches.

(2) Past and current research studies at Battelle-Columbus on Air Force projects[11, 12] have been directed toward anticipated interface problems of providing hydrogen from electrolysis cells to the Sabatier or Bosch system. The "hydrogen stripper cell" based on Pd-25Ag hydrogen-diffusion electrodes is technically an electrochemical hydrogen concentration cell which can be made to perform the function of a hydrogen pump. For example, it has been experimentally demonstrated that hydrogen stripper cell operation as an electrochemical pump to provide a hydrogen pressure of at least 20 psig is technically feasible.[12] In addition to providing a means of increasing the hydrogen pressure without the use of moving components, the "electrochemical hydrogen pump" also acts as a very efficient "electrochemical filter" to deliver pure, dry hydrogen and also acts as a positive "electrochemical valve" by providing an interruption in the

continuity of the hydrogen gas phase in the electrolyte between the cathode and anode. The hydrogen stripper cell was originally conceived for other integration aspects of the Sabatier or Bosch system but appears admirably suited for use in conjunction with open-loop operation of the water-vapor electrolysis cell with acid electrolyte. As with the conventional pump, the requirement of an electrochemical pump would be an added penalty in trade-offs. The electrochemical pump is expected to have low power consumption and light weight to compare favorably with a conventional pump. Further data are expected to be developed during the next year, on other projects at Battelle-Columbus.

(3) A related use of the hydrogen-diffusion cathode to that discussed in (2) above is based on using the Pd-25Ag cathode in the water-vapor electrolysis cell with acid electrolyte. The ability of the Pd-25Ag cathode (a thin solid metal membrane) to provide hydrogen at elevated pressure (20 psig) in a cell operating at atmospheric pressure (at the anode) is a concept ideally suited to the requirements of the water-vapor electrolysis cell operating on cabin air. However, technology developed for Pd-25Ag cathodes in alkaline electrolyte is not directly transferable to the requirements of an acid electrolyte. Some preliminary experiments were encouraging in showing that it was possible to obtain 100 percent hydrogen transmission in a free electrolyte of 85 weight percent H_3PO_4 at 60 C for about 4 hours.[12] Further experimental studies[13] of a Pd-25Ag cathode in acid electrolyte on a recently completed project for the Air Force indicated that extension of the satisfactory operating time beyond 24 hours was not readily attainable even in a free electrolyte. The problem encountered related to poisoning of the Pd-25Ag cathode by the relatively minor anodic dissolution of platinum anodes in the acid electrolyte. Further research to find suitable anode materials for acid electrolyte would be required, followed by research on matrix materials compatible with acid electrolyte and Pd-25Ag cathodes. Further research on the concept is warranted on the basis of the assumed importance to the open-loop operation of the water-vapor electrolysis cell on cabin air. However, many years of persistent research were required to perfect the Pd-25Ag cathode for use in alkaline electrolyte to achieve the present status (operation of a matrix cell with Pd-25Ag cathode and concentrated caustic at over 200 C for 2000 to 16,000 hours). Thus, the Pd-25Ag cathode does not offer a presently available solution to the hydrogen-pressure problem for acid electrolysis cells.

(4) Further study of matrix design might provide the preferred solution. Past research on the water-vapor electrolysis cell with acid electrolyte has been directed toward demonstration of extended operational capability. No research had been specifically directed toward the interface problem of hydrogen pressure as now defined. Minor improvement in matrix and cell design might be sufficient to permit open-loop operation on cabin air with hydrogen delivery pressure of 20 psig (or less as needed for feed to Sabatier or Bosch) without undue increase in cell weight or power consumption. If further evaluation of existing cell designs indicates that such a solution for open-loop operation is not immediately available, a goal for a longer range research program on the water-vapor electrolysis concept would be defined. At the present time, it appears that the research questions involve optimum matrix design and choice of acid electrolyte; these are discussed below.

BASIS FOR COMPARISON OF MATRIX DESIGNS

The water-vapor electrolysis cell can function satisfactorily (at least with small differential gas pressure) with a variety of matrix designs. For example, the silica/gel microporous PVC matrix with sulfuric acid electrolyte[1, 2] evaluated at NASA Ames and the asbestos/microporous rubber matrix with phosphoric acid electrolyte[4] evaluated at Battelle-Columbus have both demonstrated a capability of over 2000 hours of performance without adverse effect on cell electrochemical performance. A reasonable assumption is made that an asbestos/microporous rubber matrix could be used with sulfuric acid electrolyte and that a silica gel/microporous PVC matrix could be used with phosphoric acid as well as the alternative combinations which were experimentally evaluated. It seems important to consider the choice of matrix and choice of electrolyte separately. In a later section of this report, the choice of electrolyte is discussed relative to power consumption and trace contaminants. The relation of the matrix design to hydrogen pressure and other factors is discussed below.

It should be evident from the preceding discussions that the matrix design plays an important role in any discussion of hydrogen delivery pressure. Particularly, for open-loop operation, the matrix should have a high standard "bubble pressure" (in the approximate range of 0.5 to 20 psig). However, the more important criterion for matrix evaluation is the effective bubble pressure, which can best be determined in operating cells. Thus, any evaluation of matrices involving hydrogen pressure must be made under comparable (but not necessarily identical) operating conditions. A further criterion of a satisfactory matrix is a sufficiently low resistance to obtain the optimum low power consumption. A matrix can be thinner to reduce ohmic polarization up to the limit imposed by bubble pressure. Small pore size and uniformity of pore size are important for high bubble pressure. While there is probably no serious economic limitation on obtaining high-quality matrix materials, there are obviously practical physical limitations on how thin the matrix can be.

Depending on other design factors influencing the optimum design current density, there might be reason to seek a thinner matrix to reduce ohmic polarization. However, at the present time, this does not appear to be a limiting factor (less than 5 percent reduction in power possible) compared to the problem of pressure differential across the matrix for open-loop operation.

Although a low ohmic polarization might appear to be desirable for low power consumption, the total system must be considered, including power conditioning equipment. Serious consideration must be given to the degree of voltage regulation of power supplies in relation to the usual weight penalties assigned to space power systems. For example, 28 volts ± 10 percent might be available at a relatively low power penalty (lb/kw). However, this degree of voltage control might not be adequate for reasonable control of electrolysis cell performance. For example, in the hypothetical case of negligible ohmic polarization, the current/voltage characteristics of electrolysis cells are such that a 10 percent change in applied voltage could cause a tenfold change from the nominal design current density. Large fluctuations in rate of electrolysis might not be tolerable, in which case a greater degree of voltage regulation might be considered, such as 28 volts ± 1 percent. However, the weight penalty for power would be greater, or in other words, the added weight and power losses of a unit for voltage regulation would penalize the electrolysis system. Thus, in matrix design, consideration must be given to whether a reduction in ohmic polarization might not be offset by penalties for voltage control.

Perhaps the most important factor in matrix design for water-vapor electrolysis cells is the amount of electrolyte used in the initial impregnation. All available evidence indicates that the smallest amount of electrolyte possible is desirable to minimize volume changes of the electrolyte over a wide range of operating conditions (i.e., permit a wide variation in electrolyte concentration without "flooding" the electrodes or "drying out" the matrix. Therefore, the ideal matrix design appears to be a combination of porosity and thickness that minimizes electrolyte volume while permitting adequate bubble pressure and conductivity.

On the basis of the above considerations, it appears that a particular matrix design (including initial acid impregnation) should be evaluated in an operating water-vapor electrolysis cell in a manner that allows a determination of the interrelationship of the following factors:

(1) Limits of operation with respect to humidity and temperature of air

(2) Current response to transient voltage changes and steady-state voltage characteristics (i.e., current/voltage curves)

(3) Effective bubble pressure

(4) Trace-contaminant generation rates

(5) Gas purity (crossleak).

SECTION 4. REFERENCES

(1) Wydeven, T., and Johnson, R. W., "Water Electrolysis: Prospects for the Future", paper presented at Annual Aviation and Space Conference, ASME, Los Angeles, California, June 16-19, 1968.

(2) Wydeven, T., and Smith, E., "Water Vapor Electrolysis", Aerospace Medicine, October, 1967, pp 1045-1048.

(3) Conner, W. J., Greenough, B. M., and Cook, G. M., "Design and Development of a Water Vapor Electrolysis Unit", Final Report, NASA Ames Research Center, Contract NAS 2-2630, March, 1966.

(4) Clifford, J. E., "Water-Vapor Electrolysis Cell with Phosphoric Acid Electrolyte", Paper No. 670851, Aeronautic & Space Engineering and Manufacturing Meeting, Los Angeles, October 2-6, 1967.

(5) Clifford, J. E., et al., "A Water-Vapor Electrolysic Cell with Phosphoric Acid Electrolyte", NASA CR-771, June, 1967.

(6) Birdsall, C. M., Jenkins, A. C., and Spadinger, E., Anal. Chem., 24, 662-664 (1952); Treadwell and Hall, "Analytical Chemistry", Vol. 2, 8th Edition, p. 620 (1935).

(7) Lockhart, L. B., Jr., Patterson, R. L., Jr., and Anderson, W. L., "Characteristics of Air Filter Media Used for Monitoring Airborne Radioactivity", U. S. Naval Research Laboratory, NRL Report 6054, p. 6 (March 20, 1964).

(8) Armstrong, R. C., et al., "Life Support System for Space Flight of Extended Time Periods", NASA CR-614, November, 1966.

(9) Cown, W. B., Kethley, T. W., and Fincher, E. L., Appl. Microbiol., 5, 119-124 (1957).

(10) Atmospheric Contaminants in Spacecraft, Report of the Panel on Air Standards for Manned Space Flight of the Space Science Board, National Academy of Sciences, National Research Council, June, 1968.

(11) Kim, B. C., et al., "Carbon Dioxide Reduction and Water Electrolysis System", AMRL-TR-67-227, May, 1968.

(12) Clifford, J. E., et al., "Investigation of an Integrated Carbon Dioxide-Reduction and Water-Electrolysis System", AMRL-TDR-66-186, April, 1967.

(13) Kolic, E. S., and Clifford, J. E., "Water Electrolysis Cells Using Hydrogen Diffusion Cathodes", AMRL-TR-67-65, November, 1967.

(14) Kolic, E. S., and Clifford, J. E., "Water Electrolysis Cells Using Hydrogen Diffusion Cathodes", AMRL Contract No. F 33615-67-C-1515 (August, 1968).

(15) Jackson, J. K., and Blakely, R. L., "Application of Adsorption Beds to Spacecraft Life Support System", Paper No. 670842, Aeronautic and Space Engineering and Manufacturing Meeting, Society of Automotive Engineers, Los Angeles, October 2-6, 1967.

(16) Clifford, J. E., et al., "Analysis of Effects of Reduced Gravity on Electrochemical Systems", Battelle-Columbus contractor report on NAS 2-2156, December, 1967.

JEC:BCK:ESK/jvd

APPENDIX A

ANALYSIS OF HEAT- AND MASS-TRANSFER PROCESSES IN WATER-VAPOR ELECTROLYSIS

APPENDIX A

ANALYSIS OF HEAT- AND MASS-TRANSFER PROCESSES IN WATER-VAPOR ELECTROLYSIS

The purpose of this analysis is to obtain temperature and water-vapor concentration profiles set up in the flow field in the anode compartment of a matrix-type water-vapor electrolysis cell. The analysis is based upon a simplified physical model, wherein the geometry of the anode compartment is represented as a rectangular channel bounded by flat, parallel surfaces of clearance 2b, length L, and width W. The clearance is sufficiently small compared with the other two dimensions that the air flow through the anode compartment would be one dimensional, fully developed, and laminar.

Heat-Transfer Analysis

For one-dimensional, steady-state, laminar flow, assuming constant physical properties and neglecting the dissipation effect, the following equations can be derived from the conservation laws:

$$\frac{\partial u}{\partial x} = 0 \tag{1}$$

$$\frac{\partial P}{\partial x} - \mu \frac{\partial^2 u}{\partial y^2} = 0 \tag{2}$$

$$\frac{\partial P}{\partial y} = 0 \tag{3}$$

$$\rho = C_p u \frac{\partial T}{\partial x} = k\left(\frac{\partial^2 T}{\partial x^2} + \frac{\partial^2 T}{\partial y^2}\right) , \tag{4}$$

where

P = pressure, lbf/ft^2

u = flow velocity, ft/hr

T = temperature, F

k = thermal conductivity of air, Btu/(hr)(ft)(F)

μ = viscosity of air, lbf/(hr)(ft)

C_p = specific heat of air at constant pressure, Btu/(lb)(F)

ρ = density of air, lb/ft^3

x, y = rectangular coordinates, ft ($x = 0$ at entrance; $y = 0$ at the midpoint of the channel).

The following parameters are given in the problem to determine the temperature distribution:

(1) Cell dimensions

(2) Air flow rate

(3) Inlet air temperature

(4) Rate of waste-heat generation from electrolysis.

From Equations (2) and (3), it can be shown that $\frac{\partial P}{\partial x}$ = constant. Equation (2) can be integrated to obtain

$$u = \frac{1}{2\mu} \frac{dP}{dx} (b^2-y^2) \quad , \tag{5}$$

where b = one-half the channel clearance, ft.

The pressure gradient $\frac{dP}{dx}$ can now be obtained by integration of Equation (5) as follows:

$$Q = 2W \int_o^b udy = - \frac{2b^3W}{3\mu} \frac{dP}{dx}$$

$$\frac{dP}{dx} = - \frac{3\mu G}{2b^3W} \tag{6}$$

$$u = \frac{3Q}{4b^3W} (b^2-y^2) \tag{5a}$$

where Q = air flow rate/channel, ft^3/hr.

Substitution of Equations (5) and (6) into Equation (4) yields

$$\frac{3Q\rho\, C_p\, (b^2-y^2)}{4b^3W} \frac{\partial T}{\partial x} = k\left(\frac{\partial^2 T}{\partial x^2} + \frac{\partial^2 T}{\partial y^2}\right) \quad . \tag{7}$$

As a first approximation, it is assumed that the waste heat is generated uniformly from the matrix surface and, therefore, the air temperature increases linearly in the x-direction. Equation (6) then can be simplified as

$$\frac{\partial^2 T}{\partial y^2} = a\, (b^2-y^2) \quad , \tag{8}$$

where

$$a = \frac{3Q\rho\, C_p}{4k\, b^3W} \frac{\partial T}{\partial x} \quad . \tag{9}$$

Integration of Equation (8) once with respect to y yields

$$\frac{\partial T}{\partial y} = a\, (b^2y - \frac{y^3}{3}) + f_1\, (x) \quad , \tag{10}$$

where $f_1(x)$ = an arbitrary function of x.

The following two cases are of interest to the present analysis:

Case 1. The waste heat is generated from both surfaces of the channel.

Case 2. The waste heat is generated from one surface only, with other surface insulated.

Case 1. Heat Generated From Both Surfaces

Since $\frac{\partial T}{\partial y} = 0$ at y = 0 from symmetry, $f_1(x) = 0$, and Equation (10) becomes

$$\frac{\partial T}{\partial y} = a\left(b^2 y - \frac{y^3}{3}\right) \tag{10a}$$

Integration of Equation (10a) with respect to y yields

$$T = \frac{a}{12}(6b^2y^2 - y^4) + f_2(x) \quad , \tag{11}$$

where $f_2(x)$ = an arbitrary function of x.

Since the temperature is assumed to be linear in the x-direction, Equation (11) can be written as

$$T = \frac{a}{12}(6b^2y^2 - y^4) + c_1x + c_2 \tag{12}$$

where c_1, c_2 = arbitrary constants.

The arbitrary constants can be determined from the following boundary conditions:

$$\overline{T}\,(x = 0) = T_1$$

$$\overline{T}\,(x = L) = T_2$$

where

T_1, T_2 = inlet and outlet air temperatures, F

$\overline{T}$ = mean temperature of air, F

L = length of channel, ft.

The mean temperature is obtained from the temperature and velocity distributions as follows:

$$\overline{T}\,(x) = \frac{2W}{Q}\int_0^b Tudy \tag{13}$$

Substitution of Equations (5a) and (12) into Equation (13) yields

$$\overline{T} = \frac{2W}{Q}\int_0^b \left\{\frac{a}{12}(6b^2y^2-y^4) + c_1x + c_2\right\}\left\{\frac{3Q}{4b^3W}(b^2-y^2)\right\} dy$$

$$= \frac{13\ ab^4}{140} + c_1x + c_2 \quad . \tag{14}$$

From the boundary conditions, the constants can be obtained as follows:

$$c_1 = \frac{T_2-T_1}{L} \tag{15}$$

$$c_2 = T_1 - \frac{13ab^4}{140} \quad . \tag{16}$$

It can be shown from Equations (12) and (15) that

$$\frac{\partial T}{\partial x} = \frac{T_2-T_1}{L} \quad . \tag{17}$$

Substitution of Equations (15), (16), (9), and (17) into Equation (12) yields

$$T = T_1 + (T_2-T_1)\left\{\frac{Q\rho C_p}{16k\,b^3LW}(6b^2y^2-y^4) + \frac{x}{L} - \frac{39Q\,\rho\,C_p\,b}{560\,k\,LW}\right\} . \tag{18}$$

The outlet air temperature (T_2) can be eliminated from Equation (18) through an overall heat balance as follows:

$$\rho Q C_p\,(T_2-T_1) = \frac{i\,(E-1.25)LW}{0.293} \quad , \tag{19}$$

where

i = cell current density, amp/ft^2

E = cell voltage, volts.

Elimination of T_2 from Equations (18) and (19) yields the following solution for the temperature distribution of the flow field:

$$T(x,y) = T_1 + \frac{i\,(E-1.25)}{(0.293)}\left(\frac{210b^2y^2-35y^4-39b^4}{560\,kb^3} + \frac{xW}{\rho Q C_p}\right) . \tag{20}$$

The matrix temperature can be obtained from Equation (20) by setting $y = \pm b$:

$$T(x,\pm b) = T_1 + 3.41\ i\,(E-1.25)\left(\frac{136b}{560k} + \frac{Wx}{\rho Q C_p}\right) . \tag{21}$$

Case 2. Heat Generated From Bottom Surface Only

Since the top surface is insulated, $\frac{\partial T}{\partial y} = 0$ at $y = b$; and Equation (10) becomes

$$\frac{\partial T}{\partial y} = a\left(b^2 y - \frac{y^3}{3}\right) - \frac{2ab^3}{3} \tag{22}$$

The following analysis is identical to that given for Case 1:

$$T = \frac{a}{12}(6b^2y^2 - y^4) - \frac{2}{3}ab^3y + c_3x + c_4 \tag{23}$$

$$\overline{T}(x) = \frac{W}{Q}\int_{-b}^{b} Tudy$$

$$= \frac{13ab^4}{140} + c_3x + c_4 \tag{24}$$

$$c_3 = \frac{T_2 - T_1}{L} \tag{25}$$

$$c_4 = T_1 - \frac{13ab^4}{140} \tag{26}$$

$$\rho Q C_p (T_2 - T_1) = \frac{i(E-1.25)LW}{0.293} \tag{27}$$

$$T(x,y) = T_1 + 3.41\, i\,(E-1.25)\ \frac{210b^2y^2 - 35y^4 - 39b^4 - 280b^3y}{560\, b^3 k} + \frac{Wx}{\rho Q C_p}\ . \tag{28}$$

The electrolyte matrix temperature is obtained by setting y = -b in Equation (28).

$$T(x_1 - b) = T_1 + 3.41\, i\,(E-1.25)\left(\frac{416b}{560k} + \frac{Wx}{\rho Q C_p}\right) \tag{29}$$

Comparison of Equations (21) and (29) indicates that the matrix temperature is higher in Case II than in Case I as expected.

Mass-Transfer Analysis

The mass-transfer analysis to determine the concentration of water vapor in the flow field is similar to the heat-transfer analysis given for Case II. It is assumed that the flow is one-dimensional, steady state, and laminar, and that water vapor is consumed uniformly at the bottom surface of the channel so that the concentration gradient in the flow direction is linear. Conservation equations applicable to mass transfer are Equations (1), (2), (3) and the following equation:

$$u\frac{\partial w}{\partial x} = D_v\left(\frac{\partial^2 w}{\partial x^2} \quad \frac{\partial^2 w}{\partial y^2}\right) \quad , \tag{30}$$

where

w = concentration of water vapor, lb/ft^3

D_v = diffusivity of water vapor in air, ft^2/hr.

Equation (30) can be solved simultaneously with the following equations to obtain the concentration distribution:

$$\frac{\partial w}{\partial x} = \text{constant} \tag{31}$$

$$w_1 = \left[\frac{W}{Q}\int_{-b}^{b} wudy\right]_{x=0} \tag{32}$$

$$w_2 = \left[\frac{W}{Q}\int_{-b}^{b} wudy\right]_{x=L} \tag{33}$$

where

w_1, w_2 = concentration of water vapor at inlet and outlet of channel

F = 7.38×10^{-4} lb H_2O/(amp)(hr); Faraday constant.

The concentration profile is obtained as

$$w = w_1 - F_i\left(\frac{210b^2y^2-35y^4-39b^4-280b^3y}{560\ b^3\ D_v} + \frac{Wx}{Q}\right) \quad . \tag{35}$$

At the surface of the electrolyte matrix, the concentration of water vapor becomes

$$w(x_1-b) = w_1 - Fi\left(\frac{416b}{560\ D_v} + \frac{Wx}{Q}\right) \quad . \tag{36}$$

Relative Air-Flow Factor

A useful design parameter is the relative air-flow factor (n) defined as the ratio of the actual amount of water vapor supplied by the inlet air (w_1Q) to the theoretical amount of water electrolyzed. This parameter can be obtained as follows:

$$n = \frac{w_1Q}{FiLW} \quad . \tag{37}$$

The water-vapor concentration (w) can be expressed in terms of partial pressure as follows:

$$w_1 = \frac{M_2\,\rho p_1}{M_1 P} \quad , \tag{38}$$

where

p = partial pressure of water vapor, mm Hg

P = total pressure, mm Hg

M_1 = molecular weight of air; 29 lb/lb-mole

M_2 = molecular weight of water; 18 lb/lb-mole.

Substitution of Equation (38) into Equation (37) yields:

$$Q = \frac{n\ FiLWM_1P}{\rho\ M_2p_1} \tag{39}$$

By substitution of Equation (39), Equations (21), (29), and (36) can be written as follows:

$$T(x, \pm b) = T_1 + 3.41\ i\ (E-1.25)\left(\frac{136b}{560k} + \frac{M_2p_1\ x}{nM_1C_p\ Fi\ PL}\right) \tag{40}$$

$$T(x, -b) = T_1 + 3.41\ i\ (E-1.25)\left(\frac{416b}{560k} + \frac{M_2p_1\ x}{nM_1\ C_p\ Fi\ PL}\right) \tag{41}$$

$$p(x, -b) = p_1 - \frac{FiM_1P}{M_2\rho}\left(\frac{416b}{560\ D_v} + \frac{\rho M_2p_1\ x}{nM_1\ Fi\ PL}\right) . \tag{42}$$

APPENDIX B

CELL VOLTAGE CHARACTERISTICS OF THE AMES RESEARCH CENTER (ARC) MODULE

APPENDIX B

CELL VOLTAGE CHARACTERISTICS OF THE AMES RESEARCH CENTER (ARC) MODULE

INTRODUCTION

During the trace-contaminants studies (Section 2) the cells of the ARC module were wired in a series/parallel arrangement. The voltage characteristics of the individual cells could not be determined since the relative distribution of current among the four cells in each group was not known. Therefore, additional information was obtained on the ARC module by reconnecting the 12 cells in series. This permitted a determination of the individual variations in cell voltage during steady-state operation and a determination of voltage characteristics of each cell from current/voltage curves.

At the completion of the trace-contaminant studies the ARC module had accumulated 140 days of operating time and was performing satisfactorily at the 1/4-man rate at the nominal design conditions 75 F and 50 percent relative humidity. The charcoal and particulate filters were removed. For the 28 days prior to reconnecting the cells in series, the ARC module had not been operated. Therefore, the unit was operated for about 24 hours to establish steady-state conditions prior to obtaining current/voltage data. The unit was operated at 75 ± 0.5 F and a relative humidity of 48 ± 2 percent (rather than 50 ± 2 percent because of a change in the humidity-sensing element). Current/voltage data was obtained by two procedures: one cell at a time and all cells at the same time (the latter procedure has been used most often in prior studies[4, 5] at Battelle-Columbus).

Subsequently, the relative humidity was lowered to 40 ± 2 percent to provide a correlation at similar conditions with prior water-vapor electrolysis module performance (Module 2 with phosphoric acid electrolyte[4]).

EXPERIMENTAL RESULTS

Performance of Individual Cells

Table B-1 summarizes the performance of individual cells of the series-connected ARC module during the 5-day evaluation. During the first 24-hours, the module voltage was maintained at 25.8 volts (2.15 volts/cell average), corresponding to normal operation. During this period the current density slowly decreased from 37.2 amp/ft^2 to 33.5 amp/ft^2 with n = 30 ± 4 (calculated from the ΔT reading and cell voltage for cell 7). With the exception of the two end cells (1 and 12), the average cell voltage was 2.12 ± 0.07 volts (or ± 3 percent) at 33.5 amp/ft^2 (at T = 23 hours in Table B-1). The unusual performance of the end cells during the first 72 hours is believed to offer several significant clues to performance of water-vapor electrolysis cells that will be discussed in more detail in subsequent sections of this Appendix.

TABLE B-1. VOLTAGE PERFORMANCE OF ARC MODULE WITH SERIES CELL CONNECTION AT 48 PERCENT AND 40 PERCENT RELATIVE HUMIDITY (75 F)

Time (t), hours	Relative Humidity, percent	ΔT, °C	n	Current Density, amp/ft^2	Module Voltage, volts	Cell Voltages												Ozone, ppm
						1	2	3	4	5	6	7	8	9	10	11	12	
0	48 ± 2	--	--	54.9	25.80	2.178	2.112	2.100	2.189	2.158	2.108	2.185	2.173	2.050	2.242	2.065	2.288	--
1	48 ± 2	3.3	26	37.2	25.83	2.190	2.090	2.100	2.183	2.144	2.088	2.190	2.178	2.033	2.263	2.053	2.340	10.0
2	48 ± 2	2.8	30	37.2	25.80	2.195	2.073	2.108	2.172	2.117	2.086	2.172	2.166	2.040	2.264	2.061	2.373	16.5
3	48 ± 2	--	--	37.2	25.81	2.209	2.075	2.115	2.168	2.111	2.089	2.153	2.152	2.045	2.264	2.065	2.402	17.0
4	48 ± 2	2.8	28	36.8	25.76	2.207	2.075	2.117	2.156	2.106	2.090	2.096	2.134	2.050	2.255	2.070	2.413	17.5
6	48 ± 2	3.2	23	36.6	25.81	2.237	2.082	2.121	2.163	2.112	2.094	2.058	2.137	2.055	2.264	2.074	2.452	18.0
7	48 ± 2	2.6	28	36.3	25.84	2.249	2.088	2.126	2.164	2.155	2.100	2.049	2.137	2.058	2.262	2.079	2.462	--
23	48 ± 2	2.9	25	33.5	25.84	2.300	2.102	2.140	2.168	2.125	2.110	2.053	2.143	2.071	2.170	2.090	2.401	16.5
26	48 ± 2	3.2	23	33.2	25.80	2.290	2.101	2.139	2.166	2.126	2.110	2.055	2.143	2.071	2.174	2.090	2.369	18.0
32	48 ± 2	2.5	30	35.1	25.78	2.256	2.105	2.147	2.169	2.129	2.117	2.060	2.150	2.080	2.191	2.098	2.322	17.0
47	48 ± 2	2.9	26	33.2	25.82	2.258	2.104	2.143	2.167	2.134	2.115	2.060	2.147	2.076	2.191	2.096	2.357	17.0
54.4[a]	48 ± 2	--	--	34.7	--	2.172	2.105	2.146	2.164	(f)	2.118	2.061	2.148	2.082	2.200	2.099	2.141	--
54.4[b]	48 ± 2	--	--	34.7	--	2.162	2.100	2.139	2.158	--	2.113	2.056	2.141	2.076	2.184	2.093	2.118	--
54.8	48 ± 2	--	--	34.7	--	2.158	2.103	2.144	2.162	--	2.116	2.059	2.147	2.080	2.190	2.108	2.104	--
55.1[c]	48 ± 2	--	--	34.7	--	2.161	2.103	2.145	2.165	--	2.117	2.061	2.148	2.079	2.191	2.098	2.099	--
55.5	48 ± 2	2.9	26	34.7	25.45	2.156	2.105	2.138	2.157	--	2.110	2.056	2.146	2.073	2.201	2.094	2.090	6.2
71	48 ± 2	2.6	29	34.7	25.54	2.160	2.107	2.148	2.172	--	2.121	2.064	2.150	2.084	2.217	2.101	2.103	0.07
74	48 ± 2	2.5	30	34.7	25.54	2.157	2.106	2.148	2.172	--	2.119	2.064	2.151	2.083	2.218	2.101	2.104	0.07
75	40 ± 2	2.3	29	34.7	25.86	2.226	2.124	2.163	2.200	--	2.134	2.100	2.176	2.198	2.272	2.113	2.139	0.15
78	40 ± 2	3.2	25	34.7	27.60	2.430	2.233	2.213	2.305	--	2.201	2.287	2.287	2.160	2.495	2.158	2.569	17.0
80	40 ± 2	3.6	24	34.7	28.20	2.246	2.278	2.233	2.338	--	2.240	2.341	2.318	2.257	2.598	2.260	2.668	17.0
95	40 ± 2	4.3	20	30.0	28.63	2.446	2.264	2.190	2.335	--	2.241	2.342	2.317	2.381	2.650	2.561	2.610	18.0
98	40 ± 2	1.6	41	23.8	25.36	2.154	2.092	2.114	2.162	--	2.094	2.101	2.154	2.050	2.179	2.020	2.093	2.2
100	40 ± 2	2.5	27	26.0	25.54	2.182	2.097	2.126	2.187	--	2.107	2.114	2.163	2.063	2.190	2.080	2.122	0.62
102	40 ± 2	3.2	21	25.1	25.53	2.180	2.094	2.123	2.190	--	2.105	2.109	2.157	2.060	2.186	2.079	2.115	0.77
120[d]	40 ± 2	2.3	28	25.5	25.54	2.180	2.101	2.127	2.173	--	2.109	2.082	2.149	2.070	2.207	2.088	2.114	0.50
120.1[e]	40 ± 2	--	--	25.5	--	2.171	2.100	2.120	--	--	2.101	2.074	2.138	2.064	2.200	2.083	2.107	--
127.5	40 ± 2	1.6	40	25.5	25.47	2.172	2.101	2.124	--	--	2.102	2.086	2.137	2.067	2.199	2.085	2.109	0.77

(a) Voltage E_4 (Table B-3) at steady-state current density prior to C/V data.

(b) Voltage E_6 (Table B-3) immediately following C/V data 10 amp/ft^2 (E_2) and 1 amp/ft^2 (E_3) which required about 1 minute.

(c) Voltage at steady-state current density immediately prior to obtaining C/V data at 65.5 amp/ft^2 (E_1) in Table B-3 which required about 1/2 minute.

(d) Following this set of reading C/V data obtained for Table B-4 in the following sequence; steady-state current density 25.5 amp/ft^2 (E_4), 10 amp/ft^2 (E_2) and 1 amp/ft^2 (E_3) during next minute and return to 25.5 amp/ft^2 (E_6) for a few minutes and increase to 65.6 amp/ft^2 (E_1) for next 1/2 minute.

(e) Cell voltages after obtaining C/V data for Table B-4.

(f) A poor voltage lead connection prevented measurement of cell voltage.

Effect of Relative Humidity

During the last 24 hours of operation at the 48 percent relative-humidity level (up to T = 74 hours in Table B-1), the performance of all cells of the module was very good (2.14 ± 0.08 volts). However, when the relative humidity was reduced to the 40 percent level (after T = 74 hours), all cells of the module polarized to higher voltages 2.23 to 2.67 volts. The indicated decrease in calculated n value from 29-30 to 24-25 is consistent with decrease in humidity at constant air flow. The degree of polarization observed was unexpected for operation at $n \geq 20$. The cells were operated at the higher average cell voltage level of about 2.35 to 2.39 volts at 30 to 35 amp/ft^2 for about 15 hours (to T = 95 hours). The module voltage (and current density) was reduced (after T = 95 hours), with a significant decrease in polarization for the relatively small change in current density.

Ozone Generation and Cell Voltage

The last column in Table B-1 shows a correlation of ozone concentration (in ppm based on oxygen) with cell voltage (i.e., only cells at voltages above 2.15 to 2.20 volts contributing to ozone production). Further support for hypotheses regarding ozone production with sulfuric acid electrolytes was obtained from analysis of current/voltage data.

Current/Voltage Data

Tables B-2, B-3, and B-4 show the voltage characteristics of the individual cells as determined from current/voltage data. For the first 24 hours, a steady-state condition was established at about the operating design current density of 34.7 amp/ft^2 before obtaining the data in Table B-2. Thus, the cell-voltage equation as determined from relatively rapid changes in current and voltage is intended to reflect the electrolyte condition at the anode that existed for the steady-state conditions. The specific procedure used for obtaining the data in Table B-2 involving measurements for one cell at a time is believed to give accurate data for each cell. However, the method is more time consuming. The usual procedure of measuring the voltage for all cells at each current density is faster and was used for obtaining comparable data (Tables B-3 and B-4).

The voltage equation for the polarized end cells (1 and 12) as shown in Table B-2 is significant in terms of the higher-than-average "b" constant and "c" constant. It is also significant that the temporary current (and n value) changes that occurred while obtaining the current/voltage data did not eliminate the polarization of the end cells; the polarization was maintained over night from T = 32 hours to T = 47 hours as shown in Table B-1. However, for some unexplained reason, the end cells recovered from the polarized condition during the next 8 hours of operation. It is difficult to believe that the repeat measurement on Cell 10 at T = 52 hours could have precipitated the recovery of the end cells. There was no other significant change in operating conditions noted. There was no significant change in cell voltage for Cell 10 or any of the other cells while the end cells were recovering from the polarized condition. The voltage characteristics shown in Table B-3 compared with those in Table B-2 reflect the recovery of the end cells in terms of lower "b" and "c" constants.

TABLE B-2. CELL VOLTAGE CHARACTERISTICS FOR ARC MODULE OPERATING AT 48 ± 2 PERCENT RELATIVE HUMIDITY (75 F) AND 34.7 AMP/FT^2 DURING PERIOD THAT END CELLS WERE POLARIZED[a]

Cell No.	Elapsed Time, hr:min	Cell Voltages, volts: 65.6 Amp/Ft^2, E_1	10 Amp/Ft^2, E_2	1 Amp/Ft^2, E_3	Constants for Equation $E = a + b \log i + ci$: a	b	c	Cell Voltages, volts, at 34.7 Amp/Ft^2: E_4	E_5	E_6
1[b]	24:45	2.474	2.092	1.857	1.853	0.200	0.0039	2.300[b]	2.187	2.270
2[b]	28:30	2.204	1.982	1.810	1.803	0.156	0.0017	2.102[b]	2.120	2.095
3	30:00	2.256	2.013	1.825	1.823	0.172	0.0018	2.143	2.152	2.138
4	30:20	2.291	2.024	1.837	1.835	0.165	0.0024	2.166	2.173	2.159
5	30:35	2.231	2.018	1.833	1.832	0.173	0.0013	2.130	2.143	2.122
6	30:50	2.218	1.991	1.819	1.817	0.156	0.0018	2.113	2.121	2.110
7	31:00	2.156	1.940	1.780	1.778	0.144	0.0018	2.056	2.063	2.055
8	31:10	2.256	2.016	1.838	1.836	0.160	0.0020	2.144	2.152	2.140
9	31:20	2.177	1.955	1.794	1.793	0.148	0.0014	2.076	2.070	2.072
10	31:30	2.231	2.035	1.845	1.844	0.181	0.0010	2.184	2.178	2.183
11	31:40	2.196	1.973	1.806	1.804	0.151	0.0018	2.095	2.099	2.090
12	31:50	2.494	2.117	1.841	1.838	0.248	0.0031	2.321	2.336	2.302
Average		2.265	2.012	1.833	1.822	0.171	0.0020	2.155	2.157	
10[c]	52:00	2.339	2.052	1.848	1.845	0.182	0.0025	2.207	2.213	2.195

(a) See Table B-1 for operating conditions at time of measurement. Current/voltage data for one cell at a time. Readings required about 1 min and were made in the following order: the operating current density E_4 (34.7 amp/ft^2); E_1 (65 amp/ft^2); E_2 (10 amp/ft^2); E_3 (1 amp/ft^2); E_6 (34.7 amp/ft^2) constants for equation calculated from voltages E_1, E_2, and E_3.

(b) Operating current density for Cell 1 measurements, 33.2 amp/ft^2; for Cell 2, 33.9 amp/ft^2; for all other cell measurements steady-state current density at 34.7 amp/ft^2 (based on effective electrode area of 0.0765 ft^2 per cell).

(c) A repeat measurement the following day to check value of "c" constant.

TABLE B-3. VOLTAGE CHARACTERISTICS OF INDIVIDUAL CELLS OF ARC MODULE AT 48 PERCENT RELATIVE HUMIDITY[a]

Cell No.	Cell Voltages[b], volts: 65.5 Amp/Ft^2, E_1	10 Amp/Ft^2, E_2	1 Amp/Ft^2, E_3	Constants for Equation[b] $E = a + b \log i + ci$: a	b	c	Cell Voltages[b], volts at 34.7 Amp/Ft^2: E_4	E_5	E_6
1	2.282	2.025	1.837	1.835	0.166	0.0024	2.172	2.174	2.162
2	2.202	1.985	1.808	1.806	0.162	0.0017	2.105	2.115	2.100
3	2.256	2.015	1.835	1.833	0.160	0.0022	2.146	2.156	2.139
4	2.290	2.029	1.840	1.837	0.167	0.0025	2.164	2.181	2.158
5	--	--	--	--	--	--	--	--	--
6	2.220	1.998	1.818	1.816	0.164	0.0018	2.118	2.131	2.113
7	2.158	1.945	1.770	1.768	0.160	0.0017	2.061	2.074	2.056
8	2.254	2.021	1.834	1.832	0.170	0.0019	2.148	2.160	2.141
9	2.181	1.963	1.787	1.785	0.160	0.0018	2.082	2.094	2.076
10	2.330	2.045	1.840	1.837	0.181	0.0027	2.200	2.205	2.184
11	2.196	1.981	1.802	1.800	0.164	0.0017	2.099	2.112	2.093
12	2.224	1.982	1.800	1.798	0.162	0.0022	2.141	2.124	2.118
Average	2.236	1.999	1.816	1.813	0.165	0.0021	2.131	2.139	--

(a) Steady-state conditions established at time of measurement t = 54.4 hr (Table B-1):

Chamber temperature (T_1)	75 ± 0.5 F
Differential temperature (ΔT)	5.2 ± 0.5 F
Relative humidity	48 ± 2 percent
Air flow parameter (n)	26 ± 4

(b) Constants for voltage equations determined from cell voltage measurements E_1, E_2, and E_3. Equations used to calculate cell voltage (E_5) at 34.7 amp/ft^2 for comparison with measured initial value (E_4). See Table B-1 for time and footnotes (a), (b), and (c) for sequence of voltage measurements.

TABLE B-4. VOLTAGE CHARACTERISTICS OF INDIVIDUAL CELLS OF ARC MODULE AT 40 PERCENT RELATIVE HUMIDITY[a]

	Cell Voltages[b], volts			Constants for Equation[b] $E = a + b \log i + ci$			Cell Voltages[b], volts at 25.5 Amp/Ft^2		
Cell No.	65.6 Amp/Ft^2, E_1	10 Amp/Ft^2, E_2	1 Amp/Ft^2, E_3	a	b	c	E_4	E_5	E_6
1	2.349	2.071	1.863	1.861	0.188	0.0022	2.182	2.182	2.172
2	2.239	2.017	1.839	1.837	0.164	0.0016	2.105	2.109	2.101
3	2.269	2.041	1.859	1.857	0.167	0.0017	2.125	2.136	2.120
4	--	--	--	--	--	--	--	--	--
5	--	--	--	--	--	--	--	--	--
6	2.239	2.025	1.848	1.846	0.164	0.0015	2.106	2.115	2.103
7	2.220	1.990	1.807	1.805	0.168	0.0017	2.080	2.085	2.075
8	2.289	2.055	1.815	1.863	0.176	0.0016	2.146	2.152	2.139
9	2.204	1.990	1.817	1.815	0.160	0.0015	2.069	2.078	2.065
10	2.371	2.085	1.873	1.871	0.191	0.0023	2.205	2.199	2.189
11	2.222	2.005	1.831	1.829	0.160	0.0016	2.086	2.095	2.083
12	2.282	2.015	1.830	1.828	0.163	0.0024	2.113	2.119	2.107
Average	2.268	2.029	1.843	1.841	0.170	0.0018	2.121	2.126	2.112

(a) Steady-state conditions established at time of measurement t = 120 hr (Table B-1):

Chamber temperature (T_1)	75 ± 0.5 F
Differential temperature (ΔT)	4.0 ± 0.5 F
Relative humidity	40 ± 2 percent
Air flow parameter (n)	30 ± 4

(b) Constants for voltage equations determined from cell voltage measurements E_1, E_2, and E_3. Equations used to calculate cell voltage (E_5) at 25.5 amp/ft^2 for comparison with measured initial value (E_4). See Table B-1 for time and footnotes (d) and (e) for sequence of voltage measurements.

DISCUSSION OF RESULTS

Voltage Characteristics

The voltage characteristics in Table B-4 (40 percent relative humidity) compared with those in Table B-3 (48 percent relative humidity) do not show any large differences. However, the data at the lower humidity were obtained at a lower steady-state current density, which would tend to make the stready-state electrolyte conditions of temperature and concentration more similar. Considering the voltage characteristics of the cells in Table B-4, it is evident that the predicted average cell voltage increase of about 0.040 volt from 2.125 volts at 25.5 amp/ft^2 to 2.165 volts at 34.7 amp/ft^2 was greatly exceeded when cells polarized to levels of 2.24 to 2.67 volts when operated at the high current density. This suggests that a radical change must have occurred at the anode/electrolyte interface for the severely polarized cells. Since such a change would not be predicted from heat- and mass-transfer theory (Appendix A), a critical change in electrode reaction (i.e., reflected in increase in "b" constant or Tafel slope) is the more likely hypothesis. Such a hypothesis is consistent with some observations in prior studies of sulfuric acid electrolyte[3] showing two voltage levels (i.e., two different platinum anode states or electrode reactions) that appeared at about the critical anode voltage for ozone formation. The critical anode voltage was identified as about 2.07 volts, at which about 1 ppm of ozone is formed at platinized platinum sheet electrodes in an 8.5M sulfuric acid solution.[1, 10] The value of 2.07 volts corresponds to the reversible potential for the half-cell reaction in acid electrolyte:

$$H_2O + O_2 - 2H^+ + O_3 + 2e \quad .$$

The voltage equations in Tables B-3 and B-4 correlate with the above hypothesis. Assuming negligible hydrogen overvoltage for the cathodes used in the cells of the module, the voltage equation minus the ohmic polarization term (ci) represents essentially the anode voltage as a function of current density ($E = a + b \log i$). Using the equation for average cell voltage in Table B-3 (48 percent relative humidity), the estimated anode voltage at the steady-state current density of 34.7 amp/ft^{-2} is:

$$E = 1.813 + 0.165 \log (34.7) = 2.07 \text{ volts} \quad ,$$

and the average ozone concentration for all cells was 0.07 ppm at steady-state (Table B-1). Similarly, using the equation for average cell voltage in Table B-4 (40 percent relative humidity) the anode voltage at 25.5 amp/ft^2 is:

$$E = 1.841 + 0.170 (25.5) = 2.08 \text{ volts}$$

and the average ozone concentration for all cells was 0.7 ppm at steady-state (Table B-1). At the higher current density level of 34.7 amp/ft^2, the values become

$$E = 1.841 + 0.170 (34.7) = 2.10 \text{ volts}$$

and the ozone concentration was 18 ppm for the polarized condition. Possibly an increase in "b" constant associated with a new reaction (ozone) might explain some of the polarization and associated heating effects might precipitate further polarization.

There is the possibility that the extra water consumed in the ozone reaction might contribute to drying out in the matrix at the anode/electrolyte interface, leading to increased ohmic resistance (ci term). Alternatively, some of the polarization might be occurring at the cathode.

Significance of End-Cell Performance

The typical performance of the cells in response to low humidity is believed to be related to the earlier observations of unusual performance of the end cells at normal humidity (48 percent relative humidity). An effect similar to reduced humidity can be achieved by reduction in air flow (n value for series connected cells operated at constant current). While the calculated n value was relatively high (>20), it was based on only one cell of the module at the point of measurement (Cell 7). The assumption of uniform air distribution to all cells may not have been valid for the ARC module, particularly the end cells. Time did not permit a check on the relative distribution of air flow among the 12 cells. This could be done by measurement of ΔT across each cell for a series-connected module (not applicable to series/parallel arrangement). In the absence of specific data on air-flow distribution at the present time, the end-cell problem can be analyzed in terms of observed current/voltage performance.

The adverse voltage performance of end cells in the module was not expected on the basis of prior evaluation of Module 2 (phosphoric acid) at Battelle-Columbus. A possible factor is the metal end plates used in the ARC module which might contribute to increased heat loss from the ends of the module and result in cooler operating temperature for the end cells. However, the more likely hopothesis is that the air flow is restricted to the end cells because of the design of the transition ducting connecting the module to the fan. The height of the cell stack (about 6 inches) in the ARC module resulted in a sharp angle in the transition to the fan (whereas Module 2 with a cell stack height of about 3 inches had a nonangular transition to the fan). The sharp angle, by providing a smaller clearance, could restrict the air flow through the end cells. Since both modules were about the same width (6 to 7 inches), there was a sharp angle for the transition duct in the perpendicular plane. However, the restricted air flow at the ends of each cell would be the same for all cells in the module, and thus would not be readily detected. Further studies would be required to verify the hypothesis and if true, suitable corrective changes could be made in the design of the transition duct for future modules.